

Boundary-Finite Element discretization of time dependent acoustic scattering by elastic obstacles with piezoelectric behavior

Tonatiuh Sánchez-Vizuet & Francisco–Javier Sayas*

Department of Mathematical Sciences, University of Delaware, USA

{tonatiuh,fjsayas}@udel.edu

March 2, 2016

Abstract

A coupled BEM/FEM formulation for the transient interaction between an acoustic field and a piezoelectric scatterer is proposed. The scattered part of the acoustic wave is represented in terms of retarded layer potentials while the elastic displacement and electric potential are treated variationally. This results in an integro-differential system. Well posedness of a general Galerkin semi-discretization in space of the problem is shown in the Laplace domain and translated into explicit stability bounds in the time domain. Trapezoidal-Rule and BDF2 Convolution Quadrature are used in combination with matching time stepping for time discretization. Second order convergence is proven for the BDF2-based method. Numerical experiments are provided for BDF2 and Trapezoidal Rule based time evolution.

AMS Subject classification. 65R20, 65M38, 74J20, 74F10.

Keywords. Time-Domain Boundary Integral Equations, Convolution Quadrature, Scattering, Coupling BEM/FEM, Piezoelectricity.

1 Introduction

The study of the interaction between acoustic waves and elastic structures has been subject of much work in recent decades. Many of the recent modeling and computational efforts have been driven by the need to develop and improve techniques for vibration control and reduction. Passive techniques rely on the use of sound absorbing materials that dissipate the energy of the acoustic wave and have been successfully used to damp high-frequency vibrations. On the other hand, active techniques employing piezoelectric materials exploit the adaptability of the piezoelectric solid to react to the vibrations

*TSV and FJS partially funded by NSF grant DMS 1216356.

in order to cancel them. Active materials are used to provide extra control in the low frequency range.

In the frequency domain, works like [11, 12] have derived mathematical models and variational formulations suitable for numerical treatment of the process, their approach uses an effective load to model the action of the incident acoustic wave on the piezoelectric material and is geared towards a finite element solution of all the unknowns involved in the problem. In the time domain, [1] is a classic reference for finite element simulation of waves in piezoelectrics, and a thorough review of the work done on this area up until the early 2000's can be found in [9]. The propagation of plane waves in layered piezoelectric media has been addressed recently in [32, 36], using analytical methods to study the reflection and transmission of plane waves at the interface of media with different material coefficients. Within the context of dynamic crack propagation in piezoelectric solids, finite element formulations have been explored in [15, 30], while Boundary Integral Equations (BIE) have been treated in [31, 24, 17]. Time domain BIE's for a purely piezoelectric problem have been used in recent works like [16, 37], where a Nyström approach is followed for the space discretization and Convolution Quadrature is used in time. In both cases the model concerns only the propagation of the wave inside the piezoelectric material and no interaction with an acoustic wave is considered.

The present article describes, discretizes, and analyzes the complete interaction problem, considering an incident acoustic wave that interacts with a piezoelectric scatterer through coupling boundary conditions inducing an elastic wave within the piezoelectric obstacle and a scattered acoustic wave traveling in a homogeneous unbounded domain. The system of PDE's used to model the problem combines the acoustic/elastic coupling conditions presented in [22] for wave structure interaction, with the PDE's used in [12] to describe the time evolution of the relevant variables. Aiming for a Finite Element discretization of the elastic and electric variables and a boundary element treatment of the acoustic wave, the system is translated into an integro-differential problem in the Laplace domain, the analysis is carried out following the techniques systematized in [26] and originated in the seminal work [2]. Galerkin discretization in space is used for all the variables, while Convolution Quadrature combined with time stepping are used for the time evolution.

We prove that the resulting fully discrete problem is well-posed and determine stability and error bounds with explicit time dependence for the time discretization based on second order backwards differentiation formulas (BDF2). A similar study with the backward Euler method is easy to obtain, while a Trapezoidal Rule CQ method is also available [4], but knowledge of the behavior of constants with respect to time is not known at current time.

The paper is structured as follows. The general problem is presented in Section 2, where the time domain PDE model and the geometry are introduced along with the required notation and assumptions on physical parameters. Section 3 introduces the Laplace-transformed problem. Using standard BIE techniques we derive an equivalent integro-differential system and pose it variationally. The error equations satisfied by the resulting Galerkin space semi-discretization and the required elliptic projector are then presented. The core of the analysis is done in Section 4, where a slightly more general discrete system –encompassing both the discrete-in-space problem and the error equations–

is shown to be uniquely solvable by studying the variational formulation of an equivalent transmission problem; stability bounds are obtained in terms of the Laplace parameter s . The main results in the time domain are presented in Section 5, where the estimates obtained in the previous section are translated into the time domain and the system is fully discretized with BDF2-based Convolution Quadrature; for sufficiently smooth problem data second-order-in-time convergence is proven. Section 6 is dedicated to numerical experiments, some remarks pertaining the implementation of CQ and the coupling of boundary and finite elements are followed by experiments confirming convergence for the methods based in BDF2 and Trapezoidal Rule. Conclusions and possibilities for further studies are discussed in Section 7.

Background and notation. The following brackets

$$(a, b)_\Omega := \int_\Omega a b, \quad (\mathbf{a}, \mathbf{b})_\Omega := \int_\Omega \mathbf{a} \cdot \mathbf{b}, \quad (\mathbf{A}, \mathbf{B})_\Omega := \int_\Omega \mathbf{A} : \mathbf{B},$$

will be used for scalar, vector and matrix-valued real L^2 inner products. (In the latter the colon denotes the Frobenius inner product of matrices.) When using complex-valued functions the brackets will remain bilinear and conjugation will be used as needed. If Ω is an open set with Lipschitz boundary or the complementary of such a set, then $H^1(\Omega)$ is the usual Sobolev space and its norm will be denoted by $\|\cdot\|_{1,\Omega}$. The space $H^{1/2}(\partial\Omega)$ is the trace space, while $H^{-1/2}(\partial\Omega)$ is the representation of its dual when $L^2(\partial\Omega)$ is identified with its dual space. The norms of $H^{\pm 1/2}(\partial\Omega)$, both for the real and complex valued cases, will be denoted $\|\cdot\|_{\pm 1/2,\partial\Omega}$. We will finally denote $\mathbf{L}^2(\Omega) := L^2(\Omega)^d$, $\mathbf{H}^1(\Omega) := H^1(\Omega)^d$, etc., and endow these spaces with the natural product norms.

2 Problem statement

Geometric considerations. We will assume that the piezoelectric obstacle occupies a bounded, open and connected region $\Omega_- \subset \mathbb{R}^d$ with Lipschitz boundary Γ which might not be connected. The boundary will be partitioned in two non-overlapping Dirichlet and Neumann parts, open relative to Γ and such that $\Gamma = \bar{\Gamma}_D \cup \bar{\Gamma}_N$ and $\Gamma_D \neq \emptyset$.

We will adopt the convention that the unit normal vector to the boundary $\boldsymbol{\nu}$ will be taken exterior to Ω_- and as such, it will always point towards the acoustic unbounded domain $\Omega_+ := \mathbb{R}^d \setminus \bar{\Omega}_-$.

Interior variables. In the interior domain the problem variables will be the elastic displacement field \mathbf{u} and the electric potential ψ

$$\mathbf{u} : \Omega_- \times [0, \infty) \longrightarrow \mathbb{R}^d, \quad \psi : \Omega_- \times [0, \infty) \longrightarrow \mathbb{R}.$$

Differential operators in the space variables will be unsubscripted meaning, for instance, that $\nabla\psi$ is the gradient in the space variables only.

Physical parameters and tensors. We will use the following constitutive relations [35] to define the piezoelectric stress tensor $\boldsymbol{\sigma}$ and the electric displacement vector \mathbf{D}

$$\boldsymbol{\sigma} := \mathbf{C}\boldsymbol{\varepsilon}(\mathbf{u}) + \mathbf{e}\nabla\psi, \quad \mathbf{D} := \mathbf{e}^\top \boldsymbol{\varepsilon}(\mathbf{u}) - \boldsymbol{\epsilon}\nabla\psi. \quad (2.1)$$

In the above definition

$$\boldsymbol{\varepsilon}(\mathbf{u}) := \frac{1}{2} (\nabla\mathbf{u} + \nabla\mathbf{u}^\top)$$

is the linear elastic strain tensor, \mathbf{C} , \mathbf{e} , and $\boldsymbol{\epsilon}$ are the elastic compliance, piezoelectric, and dielectric tensors respectively. They encode the electric and elastic properties of the material. For a real symmetric matrix $\mathbf{M} \in \mathbb{R}_{sym}^{d \times d}$ and for a vector, $\mathbf{d} \in \mathbb{R}^d$ we define

$$\begin{aligned} (\mathbf{C}(\mathbf{x})\mathbf{M})_{ij} &:= \sum_{k,l} \mathbf{C}_{ijkl}(\mathbf{x})\mathbf{M}_{kl}, \\ (\mathbf{e}(\mathbf{x})\mathbf{d})_{ij} &:= \sum_k \mathbf{e}_{kij}\mathbf{d}_k, \\ (\mathbf{e}^\top(\mathbf{x})\mathbf{M})_k &:= \sum_{ij} \mathbf{e}_{kij}\mathbf{M}_{ij}, \\ (\boldsymbol{\epsilon}(\mathbf{x})\mathbf{d})_i &:= \sum_j \boldsymbol{\epsilon}_{ij}(\mathbf{x})\mathbf{d}_j. \end{aligned}$$

Due to physical considerations, these tensors exhibit the following symmetries [25]:

$$\mathbf{C}_{ijkl} = \mathbf{C}_{jikl} = \mathbf{C}_{klij}, \quad \mathbf{e}_{lij} = \mathbf{e}_{lji}, \quad \boldsymbol{\epsilon}_{il} = \boldsymbol{\epsilon}_{li}. \quad (2.2)$$

We will require that the components of the tensors are functions in $L^\infty(\Omega_-)$ and that for any symmetric matrix $\mathbf{M} \in \mathbb{R}_{sym}^{d \times d}$ and $\mathbf{d} \in \mathbb{R}^d$ there exist positive constants c_0 and d_0 such that for almost every $\mathbf{x} \in \Omega_-$

$$\mathbf{C}(\mathbf{x})\mathbf{M} : \mathbf{M} \geq c_0\mathbf{M} : \mathbf{M}, \quad \boldsymbol{\epsilon}(\mathbf{x})\mathbf{d} \cdot \mathbf{d} \geq d_0\mathbf{d} \cdot \mathbf{d}.$$

The density of the piezoelectric material will be denoted by ρ_Σ and will be taken to be a strictly positive function in $L^\infty(\Omega_-)$.

Exterior domain. We will assume that the unbounded domain Ω_+ surrounding the obstacle is filled with an homogeneous, isotropic and irrotational fluid with constant density ρ_f . Since the fluid is irrotational we can introduce a scalar velocity potential v such that the actual fluid velocity can be expressed as $\mathbf{v} = \nabla v$. As is standard, the total acoustic wave field v^{tot} will be the superposition of a given incident field v^{inc} and an unknown scattered field v :

$$v^{tot} = v^{inc} + v.$$

Note that even if the domain Ω_- has a cavity the total wave there will contain a non-zero contribution of the incident wave, since v^{inc} would be a solution of the problem in the absence of the scatterer. This decomposition is non-physical but mathematically meaningful. We will require that for $t \leq 0$ the incident wave has not yet reached the obstacle.

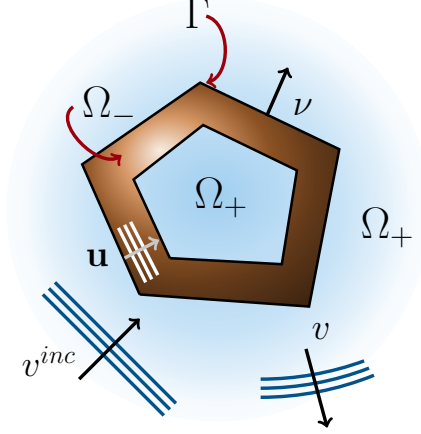


Figure 1: Scheme of the scattering geometry. The problem unknowns are the scattered acoustic wave v (defined in the unbounded region Ω_+), the induced elastic wave \mathbf{u} , and the electric potential ψ (both defined inside the obstacle Ω_-). The total elastic boundary Γ is the disjoint union of the electric Dirichlet boundary Γ_D , and the electric Neumann boundary Γ_N which are both open relative to Γ . The normal vectors $\boldsymbol{\nu}$ are exterior to the elastic domain and point towards the acoustic domain Ω_+ .

The PDE model. Under all the above considerations, and recalling the definitions (2.1), the interaction between the incident acoustic wave and the piezoelectric scatterer is governed by the following system of PDE's (see, for instance, [23, 12]):

$$\Delta v = c^{-2} v_{tt} \quad \text{in } \Omega_+ \times [0, \infty), \quad (2.3a)$$

$$\nabla \cdot \boldsymbol{\sigma} = \rho_\Sigma \mathbf{u}_{tt} \quad \text{in } \Omega_- \times [0, \infty), \quad (2.3b)$$

$$\nabla \cdot \mathbf{D} = 0 \quad \text{in } \Omega_- \times [0, \infty), \quad (2.3c)$$

$$\mathbf{u}_t \cdot \boldsymbol{\nu} + \partial_\nu v = -\alpha_d \quad \text{on } \Gamma \times [0, \infty), \quad (2.3d)$$

$$\boldsymbol{\sigma} \boldsymbol{\nu} + \rho_f v_t \boldsymbol{\nu} = -\rho_f (\beta_d)_t \boldsymbol{\nu} \quad \text{on } \Gamma \times [0, \infty), \quad (2.3e)$$

$$\mathbf{D} \cdot \boldsymbol{\nu} = \eta_d \quad \text{on } \Gamma_N \times [0, \infty), \quad (2.3f)$$

$$\psi = \mu_d \quad \text{on } \Gamma_D \times [0, \infty), \quad (2.3g)$$

with homogeneous initial conditions for v , v_t , \mathbf{u} , and \mathbf{u}_t .

The problem data is

$$\begin{aligned} \alpha_d &:= \partial_\nu v^{inc}|_\Gamma : \Gamma \times [0, \infty) \longrightarrow \mathbb{R}, & \eta_d &: \Gamma_N \times [0, \infty) \longrightarrow \mathbb{R}, \\ \beta_d &:= v^{inc}|_\Gamma : \Gamma \times [0, \infty) \longrightarrow \mathbb{R}, & \mu_d &: \Gamma_D \times [0, \infty) \longrightarrow \mathbb{R}. \end{aligned}$$

This system can be given a rigorous form using causal distributions taking values in Sobolev spaces as in [22, 26], etc. For the time being we will deal only with the Laplace transform of this system and will come back to the time domain only at the time of giving stability and error estimates.

3 A Laplace domain semidiscrete problem

In order to cast this problem rigorously we will need to define precisely the meaning of quantities on the boundary. Given $v \in H^1(\mathbb{R}^d \setminus \Gamma)$, its interior, exterior, averaged, and difference traces will be denoted by:

$$\gamma^-v, \quad \gamma^+v, \quad \{\{v\}\} := \frac{1}{2}(\gamma^-v + \gamma^+v), \quad \llbracket \gamma v \rrbracket := \gamma^-v - \gamma^+v.$$

For $(\mathbf{u}, \psi) \in \mathbf{H}^1(\Omega_-) \times H^1(\Omega_-)$ such that

$$\boldsymbol{\sigma}(\mathbf{u}, \psi) = \mathbf{C}\boldsymbol{\varepsilon}(\mathbf{u}) + \mathbf{e}\nabla\psi \in L^2(\Omega_-)^{d \times d}$$

we define the weak interior traction field in analogy to the purely elastic normal stress with the formula

$$\langle \boldsymbol{\sigma}\boldsymbol{\nu}, \gamma\mathbf{w} \rangle_\Gamma := (\mathbf{C}\boldsymbol{\varepsilon}(\mathbf{u}), \boldsymbol{\varepsilon}(\mathbf{w}))_{\Omega_-} + (\mathbf{e}\nabla\psi, \boldsymbol{\varepsilon}(\mathbf{w}))_{\Omega_-} + (\nabla \cdot \boldsymbol{\sigma}, \mathbf{w})_{\Omega_-} \quad \forall \mathbf{w} \in \mathbf{H}^1(\Omega_-).$$

In a similar fashion, for $(\mathbf{u}, \psi) \in \mathbf{H}^1(\Omega_-) \times H^1(\Omega_-)$ such that

$$\mathbf{D}(\mathbf{u}, \psi) = \mathbf{e}^\top \boldsymbol{\varepsilon}(\mathbf{u}) - \epsilon \nabla \psi \in \mathbf{L}^2(\Omega_-),$$

the weak normal electric displacement will be defined by

$$\langle \mathbf{D} \cdot \boldsymbol{\nu}, \gamma w \rangle_\Gamma := (\boldsymbol{\varepsilon}(\mathbf{u}), \mathbf{e}\nabla w)_{\Omega_-} - (\epsilon \nabla \psi, \nabla w)_{\Omega_-} + (\nabla \cdot \mathbf{D}, w)_{\Omega_-} \quad \forall w \in H^1(\Omega_-).$$

These are, respectively, elements of the dual spaces $\mathbf{H}^{-1/2}(\Gamma)$ and $H^{-1/2}(\Gamma)$. The Γ -subscripted angled bracket will be used to denote the duality product of either $H^{-1/2}(\Gamma)$ with $H^{1/2}(\Gamma)$ or $\mathbf{H}^{-1/2}(\Gamma)$ with $\mathbf{H}^{1/2}(\Gamma)$.

To deal with the Dirichlet and Neumann conditions for the electric potential, we need additional notation. The restriction to the Dirichlet boundary of the trace of a function $u \in H^1(\Omega_-)$ will be denoted by $\gamma_D u := \gamma u|_{\Gamma_D}$ and we define the function spaces

$$\begin{aligned} H^{1/2}(\Gamma_D) &:= \{\gamma_D u : u \in H^1(\Omega_-)\}, & H_D^1(\Omega_-) &:= \{u \in H^1(\Omega_-) : \gamma_D u = 0\}, \\ \tilde{H}^{1/2}(\Gamma_N) &:= \{\gamma u|_{\Gamma_N} : u \in H_D^1(\Omega_-)\}, & H^{-1/2}(\Gamma_N) &:= (\tilde{H}^{1/2}(\Gamma_N))'. \end{aligned}$$

The angled bracket $\langle \cdot, \cdot \rangle_{\Gamma_N}$ should be understood as the duality pairing of $H^{-1/2}(\Gamma_N)$ with $\tilde{H}^{1/2}(\Gamma_N)$.

Laplace domain “dynamic” problem. From this point on, we will only consider the problem in the Laplace-domain and we will use the same symbol to represent a function and its Laplace transform without ambiguity. Let $s \in \mathbb{C}_+ := \{s \in \mathbb{C} : \text{Re } s > 0\}$ and let

$$(\alpha_d, \beta_d, \eta_d, \mu_d) \in H^{-1/2}(\Gamma) \times H^{1/2}(\Gamma) \times H^{-1/2}(\Gamma_N) \times H^{1/2}(\Gamma_D)$$

be problem data. We look for $(v, \mathbf{u}, \psi) \in H^1(\Omega_+) \times \mathbf{H}^1(\Omega_-) \times H^1(\Omega_-)$ such that

$$\Delta v = (s/c)^2 v \quad \text{in } \Omega_+, \quad (3.1a)$$

$$\nabla \cdot \boldsymbol{\sigma} = \rho_\Sigma s^2 \mathbf{u} \quad \text{in } \Omega_-, \quad (3.1b)$$

$$\nabla \cdot \mathbf{D} = 0 \quad \text{in } \Omega_-, \quad (3.1c)$$

$$s\gamma \mathbf{u} \cdot \boldsymbol{\nu} + \partial_\nu^+ v = -\alpha_d \quad \text{on } \Gamma, \quad (3.1d)$$

$$\boldsymbol{\sigma}\boldsymbol{\nu} + \rho_f s \gamma^+ v \boldsymbol{\nu} = -\rho_f s \beta_d \boldsymbol{\nu} \quad \text{on } \Gamma, \quad (3.1e)$$

$$\mathbf{D} \cdot \boldsymbol{\nu} = \eta_d \quad \text{on } \Gamma_N, \quad (3.1f)$$

$$\gamma \psi = \mu_d \quad \text{on } \Gamma_D, \quad (3.1g)$$

where $\boldsymbol{\sigma}$ and \mathbf{D} are defined by (2.1).

Calderón calculus for the acoustic problem. The transmission problem

$$\begin{aligned}\Delta v - s^2 v &= 0 && \text{in } \mathbb{R}^d \setminus \Gamma, \\ \llbracket \gamma v \rrbracket &= \phi, \\ \llbracket \partial_\nu v \rrbracket &= \lambda,\end{aligned}$$

with $\lambda \in H^{-1/2}(\Gamma)$ and $\phi \in H^{1/2}(\Gamma)$, is uniquely solvable, and its solution can be expressed using the integral representation formula

$$v = S(s)\lambda - D(s)\phi. \quad (3.2)$$

The operators S and D are known as the single and double layer potentials respectively. Associated with the potentials, the following integral operators can be defined

$$\begin{aligned}V(s) &:= \{\!\!\{ \gamma \cdot \}\!\!\} S(s) = \gamma S(s), & K(s) &:= \{\!\!\{ \gamma \cdot \}\!\!\} D(s), \\ K^\top(s) &:= \{\!\!\{ \partial_\nu \cdot \}\!\!\} S(s), & W(s) &:= -\{\!\!\{ \partial_\nu \cdot \}\!\!\} D(s) = -\partial_\nu D(s).\end{aligned}$$

We recall the following useful identities

$$\partial_\nu^\pm S(s) = \mp \frac{1}{2} \mathbf{I} + K^\top(s), \quad \gamma^\pm D(s) = \pm \frac{1}{2} \mathbf{I} + K(s). \quad (3.3)$$

A coupled integro-differential system. Having defined the notation and tools we will borrow from potential theory, we can now introduce the continuous integro-differential system that will be treated numerically later on.

If (v, \mathbf{u}, ψ) is a solution of (3.1), then v can be represented as

$$v = D(s/c)\phi - S(s/c)\lambda, \quad (3.4)$$

where $\phi = \gamma^+ v$ and $\lambda = \partial_\nu^+ v$. Note that this representation can be extended to Ω_- , yielding $v \equiv 0$ in Ω_- . Therefore if we use (3.3) to write $\gamma^- v$, we arrive at

$$V(s/c)\lambda - \left(-\frac{1}{2}\mathbf{I} + K(s/c)\right)\phi = 0 \quad \text{on } \Gamma. \quad (3.5)$$

Additionally, (3.1d) and the identities (3.3) imply

$$\left(-\frac{1}{2}\mathbf{I} + K^\top(s/c)\right)\lambda + W(s/c)\phi - s\gamma \mathbf{u} \cdot \boldsymbol{\nu} = \alpha_d \quad \text{on } \Gamma. \quad (3.6)$$

Finally, (3.1e) can be written in terms of ϕ

$$\boldsymbol{\sigma} \boldsymbol{\nu} + \rho_f s \phi \boldsymbol{\nu} = -\rho_f s \beta_d \boldsymbol{\nu} \quad \text{on } \Gamma. \quad (3.7)$$

Reciprocally, if the integro-differential equations (3.5) through (4.13) are satisfied, if $(\mathbf{u}, \psi, \lambda, \phi)$ satisfies (3.1b), (3.1c), (3.1f), and (3.1g), and we define v with the representation formula (3.4), it follows that $\lambda = \partial_\nu^+ v$, $\phi = \gamma^+ v$, and we recover the system (3.1).

A variational formulation. We next define the elastodynamic bilinear form

$$b(\mathbf{u}, \mathbf{w}; s) := (\mathbf{C}\boldsymbol{\varepsilon}(\mathbf{u}), \boldsymbol{\varepsilon}(\mathbf{w}))_{\Omega_-} + s^2(\rho_\Sigma \mathbf{u}, \mathbf{w})_{\Omega_-}, \quad (3.8a)$$

and the coupled elastic-electric bilinear form

$$\begin{aligned} \mathcal{B}((\mathbf{u}, \psi), (\mathbf{w}, \varphi); s) &:= b(\mathbf{u}, \mathbf{w}; s) + (\mathbf{e}\nabla\psi, \boldsymbol{\varepsilon}(\mathbf{w}))_{\Omega_-} \\ &\quad - (\boldsymbol{\varepsilon}(\mathbf{u}), \mathbf{e}\nabla\varphi)_{\Omega_-} + (\boldsymbol{\varepsilon}\nabla\psi, \nabla\varphi)_{\Omega_-}, \end{aligned} \quad (3.8b)$$

which is bounded in $\mathbf{H}^1(\Omega_-) \times H^1(\Omega_-)$. We also collect all the integral operators in (3.5)-(3.6) in a single matrix of operators

$$\mathbb{D}(s) := \begin{bmatrix} \mathbf{V}(s) & +\frac{1}{2}\mathbf{I} - \mathbf{K}(s) \\ -\frac{1}{2}\mathbf{I} + \mathbf{K}^\top(s) & \mathbf{W}(s) \end{bmatrix} : H^{-1/2}(\Gamma) \times H^{1/2}(\Gamma) \rightarrow H^{1/2}(\Gamma) \times H^{-1/2}(\Gamma). \quad (3.8c)$$

For the sake of notational simplicity, we will write $\mathbb{D}(s)(\lambda, \phi)$ for the action of $\mathbb{D}(s)$ on the column vector $(\lambda, \phi)^\top$. We now present the continuous variational formulation of the problem which reads:

Given data $(\alpha_d, \beta_d, \eta_d, \mu_d) \in H^{-1/2}(\Gamma) \times H^{1/2}(\Gamma) \times H^{-1/2}(\Gamma_N) \times H^{1/2}(\Gamma_D)$, find $(\mathbf{u}, \psi, \lambda, \phi) \in \mathbf{H}^1(\Omega_-) \times H^1(\Omega_-) \times H^{-1/2}(\Gamma) \times H^{1/2}(\Gamma)$ such that

$$\gamma_D \psi = \mu_d, \quad (3.9a)$$

and for all $(\mathbf{w}, \varphi) \in \mathbf{H}^1(\Omega_-) \times H^1(\Omega_-)$ and $(\xi, \chi) \in H^{-1/2}(\Gamma) \times H^{1/2}(\Gamma)$

$$\mathcal{B}((\mathbf{u}, \psi), (\mathbf{w}, \varphi); s) + \rho_f s \langle \phi, \gamma \mathbf{w} \cdot \boldsymbol{\nu} \rangle_\Gamma = -\rho_f s \langle \beta_d, \gamma \mathbf{w} \cdot \boldsymbol{\nu} \rangle_\Gamma + \langle \eta_d, \gamma \varphi \rangle_{\Gamma_N}, \quad (3.9b)$$

$$-s \langle \gamma \mathbf{u} \cdot \boldsymbol{\nu}, \chi \rangle_\Gamma + \langle \mathbb{D}(s/c)(\lambda, \phi), (\xi, \chi) \rangle_\Gamma = \langle \alpha_d, \chi \rangle_\Gamma. \quad (3.9c)$$

Discrete formulation. In order to discretize the system (3.9) a few definitions are in order. We consider finite dimensional subspaces

$$\mathbf{V}_h \subseteq \mathbf{H}^1(\Omega_-), \quad V_h \subseteq H^1(\Omega_-), \quad V_{h,D} := V_h \cap H_D^1(\Omega_-), \quad X_h \subseteq H^{-1/2}(\Gamma), \quad Y_h \subseteq H^{1/2}(\Gamma).$$

(Note that, following [26], the theoretical treatment of the s -dependent discrete problem only uses that these spaces are closed. This has the advantage of simultaneously providing a well-posedness analysis of the continuous problem.) It will be assumed that the set

$$\mathbf{M} := \{ \mathbf{m} \in \mathbf{H}^1(\Omega_-) : \boldsymbol{\varepsilon}(\mathbf{m}) = 0 \quad \forall \mathbf{w} \in \mathbf{H}^1(\Omega_-) \}$$

of elastic rigid motions is always contained in \mathbf{V}_h . In the discrete case, the Dirichlet boundary condition will be approximated in the space $\gamma_D V_h := \{ \gamma_D v^h : v^h \in V_h \}$. With all this in mind, we can now pose the discrete counterpart of (3.9).

Given problem data $(\alpha_d, \beta_d, \eta_d, \mu_d^h) \in H^{-1/2}(\Gamma) \times H^{1/2}(\Gamma) \times H^{-1/2}(\Gamma_N) \times \gamma_D V_h$, find $(\mathbf{u}^h, \psi^h, \lambda^h, \phi^h) \in \mathbf{V}_h \times V_h \times Y_h \times X_h$ such that

$$\gamma_D \psi^h = \mu_d^h, \quad (3.10a)$$

and for all $(\mathbf{w}, \varphi) \in \mathbf{V}_h \times V_{h,D}$ and $(\xi, \chi) \in X_h \times Y_h$

$$\mathcal{B}((\mathbf{u}^h, \psi^h), (\mathbf{w}, \varphi); s) + \rho_f s \langle \phi^h, \gamma \mathbf{w} \cdot \boldsymbol{\nu} \rangle_\Gamma = -\rho_f s \langle \beta_d, \gamma \mathbf{w} \cdot \boldsymbol{\nu} \rangle_\Gamma + \langle \eta_d, \gamma \varphi \rangle_{\Gamma_N}, \quad (3.10b)$$

$$-s \langle \gamma \mathbf{u}^h \cdot \boldsymbol{\nu}, \chi \rangle_\Gamma + \langle \mathbb{D}(s/c)(\lambda^h, \phi^h), (\xi, \chi) \rangle_\Gamma = \langle \alpha_d, \chi \rangle_\Gamma. \quad (3.10c)$$

A short-hand form of (3.10c) can be given using polar sets. If U_h is a subspace of the Hilbert space U , the expression $v \in U_h^\circ \subset U'$ (v is in the polar set of U_h), will be shorthand for

$$\langle v, u \rangle_{U' \times U} = 0 \quad \forall u \in U_h.$$

We can then shorten (3.10c) as

$$-(0, s\gamma \mathbf{u}^h \cdot \boldsymbol{\nu}) + \mathbb{D}(s/c)(\lambda^h, \phi^h) - (0, \alpha_d) \in X_h^\circ \times Y_h^\circ \equiv (X_h \times Y_h)^\circ.$$

Trace liftings. By definition, the restriction of the trace to the Dirichlet boundary

$$\gamma_D : H^1(\Omega_-) \longrightarrow H^{1/2}(\Gamma_D)$$

is a surjective operator, and so is

$$\gamma_{h,D} := \gamma_D|_{V_h} : V_h \longrightarrow \gamma_D V_h.$$

Note that there exists a bounded right-inverse of γ_D (or lifting) which will be denoted by γ_D^\dagger . For the discrete counterpart, the existence of a right-inverse of $\gamma_{h,D}$ that is bounded uniformly in h will be assumed (see [13]) and will be denoted $\gamma_{h,D}^\dagger$.

An elliptic projector. A projection operator will be required in order to project the solid-electric component of the exact solution on the discrete space. Given $(\mathbf{u}, \psi, \mu_d^h) \in \mathbf{H}^1(\Omega_-) \times H_D^1(\Omega_-) \times \gamma_D V_h$ we will write $(\mathbf{P}_h \mathbf{u}, \mathbf{P}_h \psi) \in \mathbf{V}_h \times V_{h,D}$ to denote the pair satisfying

$$\gamma_D \mathbf{P}_h \psi = \mu_d^h, \quad (3.11a)$$

the discrete variational equation

$$\mathcal{B}((\mathbf{P}_h \mathbf{u}, \mathbf{P}_h \psi), (\mathbf{w}, \varphi); 0) = \mathcal{B}((\mathbf{u}, \psi), (\mathbf{w}, \varphi); 0) \quad \forall (\mathbf{w}, \varphi) \in \mathbf{V}_h \times V_{h,D}, \quad (3.11b)$$

and the ‘grounding condition’

$$(\mathbf{P}_h \mathbf{u}, \mathbf{m})_{\Omega_-} = (\mathbf{u}, \mathbf{m})_{\Omega_-} \quad \forall \mathbf{m} \in \mathbf{M}. \quad (3.11c)$$

Note that the bilinear form in (3.11) does not contain the s -dependent term (we have set $s = 0$), which is the kinetic part of the elastic-electric bilinear form \mathcal{B} . Note also that both $\mathbf{P}_h \mathbf{u}$ and $\mathbf{P}_h \psi$ depend on (\mathbf{u}, ψ) as well as on the discrete data μ_d^h . We will keep the simplified (and somewhat misleading) notation for the sake of simplicity. The next lemma shows that this elliptic projection is quasioptimal.

Lemma 3.1. *Problem (3.11) is uniquely solvable and there exists $C > 0$ such that*

$$\begin{aligned} \|\mathbf{u} - \mathbf{P}_h \mathbf{u}\|_{1,\Omega_-} + \|\psi - \mathbf{P}_h \psi\|_{1,\Omega_-} \leq C & \left(\inf_{\mathbf{w} \in \mathbf{V}_h} \|\mathbf{u} - \mathbf{w}\|_{1,\Omega_-} + \inf_{\varphi \in V_h} \|\psi - \varphi\|_{1,\Omega_-} \right. \\ & \left. + \|\gamma_D \psi - \mu_d^h\|_{1/2,\Gamma} \right). \end{aligned}$$

Proof. The bilinear form $\mathcal{B}(\cdot, \cdot; 0)$ is coercive in the space

$$\{\mathbf{u} \in \mathbf{H}^1(\Omega_-) : (\mathbf{u}, \mathbf{m})_{\Omega_-} = 0 \quad \forall \mathbf{m} \in \mathbf{M}\} \times H_D^1(\Omega_-),$$

as follows from the second Korn and Poincaré-Friedrichs inequalities, since $\Gamma_D \neq \emptyset$. If $\{\mathbf{m}_i : i = 1, \dots, N_d\}$ is a basis for the space \mathbf{M} , then a simple compactness argument shows that the bilinear form

$$\mathcal{B}((\mathbf{u}, \psi), (\mathbf{w}, \varphi); 0) + \sum_{i=1}^{N_d} (\mathbf{u}, \mathbf{m}_i)_{\Omega_-} (\mathbf{w}, \mathbf{m}_i)_{\Omega_-}$$

is coercive in $H^1(\Omega_-) \times H_D^1(\Omega_-)$. Therefore, when $\mu_D^h = 0$, it is simple to see that (3.11) is just a Galerkin discretizations in $\mathbf{V}_h \times V_{h,D}$ of a coercive problem, and therefore a Céa estimate holds. The consideration of non-homogeneous boundary conditions, leading to an estimate like the one on the statement of the Lemma, can be approached using standard arguments based on the hypothesis of the existence of an h -uniform lifting of $\gamma_{h,D}$ [13]. \square

Error equations. The error will be analyzed using the variables

$$\begin{aligned} \mathbf{e}_{\mathbf{u}}^h &:= \mathbf{P}_h \mathbf{u} - \mathbf{u}^h, & e_{\psi}^h &:= \mathbf{P}_h \psi - \psi^h, \\ e_{\lambda}^h &:= \lambda - \lambda^h, & e_{\phi}^h &:= \phi - \phi^h, \end{aligned}$$

which satisfy

$$\gamma_D e_h^{\psi} = 0, \tag{3.12a}$$

and for all $(\mathbf{w}, \varphi) \in \mathbf{V}_h \times V_{h,D}$

$$\mathcal{B}((\mathbf{e}_{\mathbf{u}}^h, e_{\psi}^h), (\mathbf{w}, \varphi); s) + \rho_f s \langle e_{\phi}^h, \gamma \mathbf{w} \cdot \boldsymbol{\nu} \rangle_{\Gamma} - s^2 (\rho_{\Sigma} (\mathbf{P}_h \mathbf{u} - \mathbf{u}), \mathbf{w})_{\Omega_-} = 0, \tag{3.12b}$$

$$-(0, s \gamma \mathbf{e}_{\mathbf{u}}^h \cdot \boldsymbol{\nu}) + \mathbb{D}(s/c)(e_{\lambda}^h, e_{\phi}^h) - (0, s \gamma (\mathbf{P}_h \mathbf{u} - \mathbf{u}) \cdot \boldsymbol{\nu}) \in X_h^{\circ} \times Y_h^{\circ}. \tag{3.12c}$$

4 Laplace domain analysis

We consider a slightly more general problem from which both stability and error estimates for (3.10) will be obtained. Data are

$$(\alpha_d, \beta_d, \eta_d, \mu_d^h) \in H^{-1/2}(\Gamma) \times H^{1/2}(\Gamma) \times H^{-1/2}(\Gamma_N) \times \gamma_D V_h, \tag{4.1a}$$

and

$$(\boldsymbol{\theta}_d, \theta_d, \lambda_d, \phi_d) \in \mathbf{H}^1(\Omega_-) \times L^2(\Gamma) \times H^{-1/2}(\Gamma) \times H^{1/2}(\Gamma), \tag{4.1b}$$

and we look for

$$(\widehat{\mathbf{u}}^h, \widehat{\psi}^h) \in \mathbf{V}_h \times V_{h,D} \quad \text{and} \quad (\widehat{\lambda}^h, \widehat{\phi}^h) \in H^{-1/2}(\Gamma) \times H^{1/2}(\Gamma)$$

such that for all $(\mathbf{w}, \varphi) \in \mathbf{V}_h \times V_{h,D}$

$$\gamma_D \widehat{\psi}^h = \mu_d^h, \tag{4.2a}$$

$$\begin{aligned} \mathcal{B}((\widehat{\mathbf{u}}^h, \widehat{\psi}^h), (\mathbf{w}, \varphi); s) + \rho_f s \langle \widehat{\phi}^h, \gamma \mathbf{w} \cdot \boldsymbol{\nu} \rangle_\Gamma = & -\rho_f s \langle \beta_d, \gamma \mathbf{w} \cdot \boldsymbol{\nu} \rangle_\Gamma + \langle \eta_d, \gamma \varphi \rangle_{\Gamma_N} \\ & + s^2 (\rho_\Sigma \boldsymbol{\theta}_d, \mathbf{w})_{\Omega_-}, \end{aligned} \tag{4.2b}$$

$$-(0, s \gamma \widehat{\mathbf{u}}^h \cdot \boldsymbol{\nu}) + \mathbb{D}(s/c)(\widehat{\lambda}^h, \widehat{\phi}^h) - (0, \alpha_d + s \theta_d) \in X_h^\circ \times Y_h^\circ, \tag{4.2c}$$

$$(\widehat{\lambda}^h, \widehat{\phi}^h) - (\lambda_d, \phi_d) \in X_h \times Y_h. \tag{4.2d}$$

Note that if the first group of data (4.1a) is set to be zero and we take

$$(\boldsymbol{\theta}_d, \theta_d, \lambda_d, \phi_d) = (\mathbf{P}_h \mathbf{u} - \mathbf{u}, \gamma(\mathbf{P}_h \mathbf{u} - \mathbf{u}) \cdot \boldsymbol{\nu}, \lambda, \phi),$$

the system (4.2) reduces to the error equations (3.12), while if the second group of data (4.1b) is identically zero then the discrete equations (3.10) are recovered.

Two equivalent problems. Using the Galerkin equations (4.2) as the starting point, the analysis will proceed as in [26] by finding an equivalent transmission problem that can then be studied variationally. Solvability will then be established for the variational formulation and the stability constants will be obtained from the variational problem as well.

Proposition 4.1 (Transmission problem). *If $(\widehat{\mathbf{u}}^h, \widehat{\psi}^h, \widehat{\lambda}^h, \widehat{\phi}^h)$ solves (4.2), and*

$$\widehat{v}^h := \mathbb{D}(s/c) \widehat{\phi}^h - \mathbb{S}(s/c) \widehat{\lambda}^h, \tag{4.3}$$

then $(\widehat{v}^h, \widehat{\mathbf{u}}^h, \widehat{\psi}^h) \in H^1(\mathbb{R}^d \setminus \Gamma) \times \mathbf{V}_h \times V_{h,D}$ satisfies for all $(\mathbf{w}, \varphi) \in \mathbf{V}_h \times V_{h,D}$

$$-\Delta \widehat{v}^h + (s/c)^2 \widehat{v}^h = 0 \quad \text{in } \mathbb{R}^d \setminus \Gamma, \tag{4.4a}$$

$$\gamma_D \widehat{\psi}^h = \mu_d^h \quad \text{on } \Gamma, \tag{4.4b}$$

$$\begin{aligned} \mathcal{B}((\widehat{\mathbf{u}}^h, \widehat{\psi}^h), (\mathbf{w}, \varphi); s) - \rho_f s \langle \llbracket \gamma \widehat{v}^h \rrbracket, \gamma \mathbf{w} \cdot \boldsymbol{\nu} \rangle_\Gamma = & -\rho_f s \langle \beta_d, \gamma \mathbf{w} \cdot \boldsymbol{\nu} \rangle_\Gamma + \langle \eta_d, \gamma \varphi \rangle_{\Gamma_N} \\ & + s^2 (\rho_\Sigma \boldsymbol{\theta}_d, \mathbf{w})_{\Omega_-}, \end{aligned} \tag{4.4c}$$

$$-(0, s \gamma \widehat{\mathbf{u}}^h \cdot \boldsymbol{\nu}) + (\gamma^- \widehat{v}^h, \partial_\nu^+ \widehat{v}^h) - (0, \alpha_d + s \theta_d) \in X_h^\circ \times Y_h^\circ, \tag{4.4d}$$

$$(\llbracket \partial_\nu \widehat{v}^h \rrbracket + \lambda_d, \llbracket \gamma \widehat{v}^h \rrbracket + \phi_d) \in X_h \times Y_h. \tag{4.4e}$$

Conversely, given a solution triplet $(\widehat{v}^h, \widehat{\mathbf{u}}^h, \widehat{\psi}^h)$ to (4.4) and defining $\widehat{\lambda}^h := -\llbracket \partial_\nu \widehat{v}^h \rrbracket$, and $\widehat{\phi}^h := -\llbracket \gamma \widehat{v}^h \rrbracket$, the functions $(\widehat{\mathbf{u}}^h, \widehat{\psi}^h, \widehat{\lambda}^h, \widehat{\phi}^h)$ solve (4.2).

Proof. Given a solution of (4.2) and defining \widehat{v}^h as in (4.3), it follows from the properties of the layer potentials that (4.4a) is satisfied. Another consequence of this definition is that $\llbracket \gamma \widehat{v}^h \rrbracket = -\widehat{\phi}^h$ and $\llbracket \partial_\nu \widehat{v}^h \rrbracket = -\widehat{\lambda}^h$, which shows that equations (4.4c) and (4.4e) follow

readily from (4.2b) and (4.2d) by substitution of the above terms. Moreover, using the identities (3.3) to compute $\gamma^-\widehat{v}^h$ and $\partial_\nu^+\widehat{v}^h$, it can be seen that (4.2c) and (4.4d) are equivalent.

The proof of the converse is very similar and requires only to observe that (4.4a) allows for the layer potential representation of the acoustic field

$$\widehat{v}^h = D(s/c)\gamma^+\widehat{v}^h - S(s/c)\partial_\nu^+\widehat{v}^h.$$

Thus, defining $\widehat{\lambda}^h$ and $\widehat{\phi}^h$ as in the statement all the above arguments can be repeated to show that equations (4.2) hold. \square

The system (4.4) can now be treated variationally. To do this we introduce the space

$$V_h^* := \{w \in H^1(\mathbb{R}^d \setminus \Gamma) : \llbracket \gamma w \rrbracket \in Y_h, \text{ and } \gamma^- w \in X_h^\circ\}.$$

The following proposition gives the equivalent variational formulation from which the solvability and stability bounds of the entire problem will be deduced.

Proposition 4.2 (Variational formulation). *Consider the bilinear and linear forms*

$$\begin{aligned} \mathcal{A}((v, \mathbf{u}, \psi), (w, \mathbf{w}, \varphi); s) &:= (\nabla v, \nabla w)_{\mathbb{R}^d \setminus \Gamma} + (s/c)^2(v, w)_{\mathbb{R}^d \setminus \Gamma} \\ &\quad + \mathcal{B}((\mathbf{u}, \psi), (\mathbf{w}, \varphi); s) \\ &\quad + \rho_f s \langle \gamma \mathbf{u} \cdot \boldsymbol{\nu}, \llbracket \gamma w \rrbracket \rangle_\Gamma - \rho_f s \langle \llbracket \gamma v \rrbracket, \gamma \mathbf{w} \cdot \boldsymbol{\nu} \rangle_\Gamma, \end{aligned}$$

$$\begin{aligned} \ell((w, \mathbf{w}, \varphi); s) &:= - \langle \lambda_d, \gamma^- w \rangle_\Gamma + \langle \alpha_d + s\theta_d, \llbracket \gamma w \rrbracket \rangle_\Gamma \\ &\quad + s^2(\rho_\Sigma \boldsymbol{\theta}_d, \mathbf{w})_{\Omega_-} - \rho_f s \langle \beta_d, \gamma \mathbf{w} \cdot \boldsymbol{\nu} \rangle_\Gamma \\ &\quad + \langle \eta_d, \gamma \varphi \rangle_{\Gamma_N}. \end{aligned}$$

The system (4.4) is equivalent to the problem of finding $(\widehat{v}^h, \widehat{\mathbf{u}}^h, \widehat{\psi}^h) \in H^1(\mathbb{R}^d \setminus \Gamma) \times \mathbf{V}_h \times V_{h,D}$ such that

$$\gamma_D \widehat{\psi}^h = \mu_d^h, \tag{4.5a}$$

$$(\llbracket \gamma \widehat{v}^h \rrbracket + \phi_d, \gamma^- \widehat{v}^h) \in Y_h \times X_h^\circ, \tag{4.5b}$$

$$\mathcal{A}((\widehat{v}^h, \widehat{\mathbf{u}}^h, \widehat{\psi}^h), (w, \mathbf{w}, \varphi); s) = \ell((w, \mathbf{w}, \varphi); s) \quad \forall (w, \mathbf{w}, \varphi) \in V_h^* \times \mathbf{V}_h \times V_{h,D}. \tag{4.5c}$$

Proof. Given a solution $(\widehat{v}^h, \widehat{\mathbf{u}}^h, \widehat{\psi}^h)$ to (4.4) we note that (4.5b) is equivalent to the first component of (4.4d) and the second component of (4.4e). Moreover, testing $\partial_\nu^+ \widehat{v}$ with $\llbracket \gamma w \rrbracket$ for $w \in V_h^*$, we obtain

$$\begin{aligned} \langle \partial_\nu^+ \widehat{v}^h, \llbracket \gamma w \rrbracket \rangle_\Gamma &= \langle \partial_\nu^- \widehat{v}^h, \gamma^- w \rangle_\Gamma - \langle \partial_\nu^+ \widehat{v}^h, \gamma^+ w \rangle_\Gamma - \langle \llbracket \partial_\nu \widehat{v}^h \rrbracket, \gamma^- w \rangle_\Gamma \\ &= (\nabla \widehat{v}^h, \nabla w)_{\mathbb{R}^d \setminus \Gamma} + (\Delta \widehat{v}^h, w)_{\mathbb{R}^d \setminus \Gamma} - \langle \llbracket \partial_\nu \widehat{v}^h \rrbracket, \gamma^- w \rangle_\Gamma \\ &= (\nabla \widehat{v}^h, \nabla w)_{\mathbb{R}^d \setminus \Gamma} + (s/c)^2(\widehat{v}^h, w)_{\mathbb{R}^d \setminus \Gamma} - \langle \llbracket \partial_\nu \widehat{v}^h \rrbracket + \lambda_d, \gamma^- w \rangle_\Gamma + \langle \lambda_d, \gamma^- w \rangle_\Gamma \\ &= (\nabla \widehat{v}^h, \nabla w)_{\mathbb{R}^d \setminus \Gamma} + (s/c)^2(\widehat{v}^h, w)_{\mathbb{R}^d \setminus \Gamma} + \langle \lambda_d, \gamma^- w \rangle_\Gamma, \end{aligned} \tag{4.6}$$

where we have used the definition of the weak normal derivative $\partial_\nu^\pm \widehat{v}^h$ in conjunction with equations (4.4a), (4.4d) and the first component of (4.4e). Therefore, for $w \in V_h^*$ it follows from the second component of (4.4e) and (4.6) that

$$(\nabla \widehat{v}^h, \nabla w)_{\mathbb{R}^d \setminus \Gamma} + (s/c)^2 (\widehat{v}^h, w)_{\mathbb{R}^d \setminus \Gamma} + \langle \lambda_d, \gamma^- w \rangle_\Gamma + \langle s\gamma \widehat{\mathbf{u}}^h \cdot \boldsymbol{\nu} + \alpha_d + s\theta_d, \llbracket \gamma w \rrbracket \rangle_\Gamma = 0.$$

This expression in combination with (4.4c) are equivalent to (4.5c).

To verify the converse statement, we expand the bilinear form in (4.5c) and rewrite it in terms of the interior/exterior normal derivatives of \widehat{v}^h and its Laplacian to show that

$$\begin{aligned} 0 &= (\Delta \widehat{v}^h, w)_{\Omega_-} - (s/c)^2 (\widehat{v}^h, w)_{\Omega_-} \\ &\quad + \mathcal{B}((\widehat{\mathbf{u}}^h, \widehat{\psi}^h), (\mathbf{w}, \varphi); s) - s^2 (\rho_\Sigma \boldsymbol{\theta}_d, \mathbf{w})_{\Omega_-} - \rho_f s \langle \llbracket \gamma \widehat{v}^h \rrbracket + \beta_d, \gamma \mathbf{w} \cdot \boldsymbol{\nu} \rangle_\Gamma - \langle \eta_d, \gamma \varphi \rangle_{\Gamma_N} \\ &\quad + \langle \rho_f s \gamma \widehat{\mathbf{u}}^h \cdot \boldsymbol{\nu} + \alpha_d + s\theta_d, \llbracket \gamma w \rrbracket \rangle_\Gamma \\ &\quad + \langle \llbracket \partial_\nu \widehat{v}^h \rrbracket + \lambda_d, \gamma^- w \rangle_\Gamma. \end{aligned}$$

Once the equation is rewritten in this form, it is enough to notice that the mapping

$$\begin{aligned} V_h^* \times \mathbf{V}_h \times V_{h,D} &\longrightarrow V_h^* \times \mathbf{V}_h \times V_{h,D} \times X_h^\circ \times Y_h \\ (w, \mathbf{w}, \varphi) &\longmapsto (w, \mathbf{w}, \varphi, \gamma^- w, \llbracket \gamma w \rrbracket) \end{aligned}$$

is surjective to conclude that every line of the above expression must vanish independently, which implies –line by line– equations (4.4a), (4.4c), the second component of (4.4d), and the first component of (4.4e). The boundary condition (4.4b) is given and the remaining two components of (4.4d) and (4.4e) are imposed strongly by the choice of function spaces. \square

Well-posedness and stability. For $s \in \mathbb{C}_+$ we write

$$\sigma := \operatorname{Re} s > 0, \quad \underline{\sigma} := \min\{\sigma, 1\}.$$

To shorten some of the forthcoming expressions, we will denote:

$$\begin{aligned} \|(v, \mathbf{u}, \psi)\|_1^2 &:= \rho_f \|\nabla v\|_{\mathbb{R}^d \setminus \Gamma}^2 + \rho_f c^{-2} \|v\|_{\mathbb{R}^d}^2 \\ &\quad + (\mathbf{C}\boldsymbol{\varepsilon}(\mathbf{u}), \boldsymbol{\varepsilon}(\bar{\mathbf{u}}))_{\Omega_-} + (\rho_\Sigma \mathbf{u}, \bar{\mathbf{u}})_{\Omega_-} + (\boldsymbol{\varepsilon} \nabla \psi, \nabla \bar{\psi})_{\Omega_-}. \end{aligned}$$

Following the program laid out in [26], we define the energy norm

$$\begin{aligned} \|(v, \mathbf{u}, \psi)\|_{|s|}^2 &:= \rho_f \|\nabla v\|_{\mathbb{R}^d \setminus \Gamma}^2 + \rho_f c^{-2} \|sv\|_{\mathbb{R}^d}^2 \\ &\quad + (\mathbf{C}\boldsymbol{\varepsilon}(\mathbf{u}), \boldsymbol{\varepsilon}(\bar{\mathbf{u}}))_{\Omega_-} + \|s\sqrt{\rho_\Sigma} \mathbf{u}\|_{\Omega_-}^2 + (\boldsymbol{\varepsilon} \nabla \psi, \nabla \bar{\psi})_{\Omega_-}, \end{aligned}$$

which includes kinetic and potential contributions from the acoustic and elastic fields, and the potential energy from the dielectric field. Notice that since $\Gamma_D \neq \emptyset$ this defines a norm in $V_h^* \times \mathbf{V}_h \times V_{h,D}$. A simple computation shows that

$$\underline{\sigma} \|(v, \mathbf{u}, \psi)\|_1 \leq \|(v, \mathbf{u}, \psi)\|_{|s|} \leq \frac{|s|}{\underline{\sigma}} \|(v, \mathbf{u}, \psi)\|_1. \quad (4.7)$$

Proposition 4.3 (Well-posedness). *Problem (4.5) is uniquely solvable for any*

$$\begin{aligned} (\alpha_d, \beta_d, \eta_d, \mu_d^h) &\in H^{-1/2}(\Gamma) \times H^{1/2}(\Gamma) \times H^{-1/2}(\Gamma_N) \times \gamma_D V_h, \\ (\boldsymbol{\theta}_d, \theta_d, \lambda_d, \phi_d) &\in \mathbf{H}^1(\Omega_-) \times L^2(\Gamma) \times H^{-1/2}(\Gamma) \times H^{1/2}(\Gamma), \end{aligned}$$

and $s \in \mathbb{C}_+$. Moreover, there exists $C > 0$ independent of h and s such that

$$\|(\widehat{v}^h, \widehat{\mathbf{u}}^h, \widehat{\psi}^h)\|_1 + \|\widehat{\phi}^h\|_{1/2, \Gamma} \leq C \frac{|s|}{\sigma \underline{\sigma}^2} A(\text{data}, s), \quad (4.8a)$$

$$\|\widehat{\lambda}^h\|_{-1/2, \Gamma} \leq C \frac{|s|^{3/2}}{\sigma \underline{\sigma}^{3/2}} A(\text{data}, s), \quad (4.8b)$$

where

$$\begin{aligned} A(\text{data}, s) &:= \|\alpha_d\|_{-1/2, \Gamma} + \|s\beta_d\|_{1/2, \Gamma} + \|\eta_d\|_{-1/2, \Gamma} + \|s\mu_d^h\|_{1/2, \Gamma} \\ &\quad + \|s^2\boldsymbol{\theta}_d\|_{\Omega_-} + \|s\theta_d\|_{\Gamma} + \|\lambda_d\|_{-1/2, \Gamma} + \|s\phi_d\|_{1/2, \Gamma}. \end{aligned}$$

Proof. It is easy to check that

$$\left| \operatorname{Re} \bar{s} \mathcal{A} \left((v, \mathbf{u}, \psi), \overline{(v, \mathbf{u}, \psi)}; s \right) \right| = \sigma \|(v, \mathbf{u}, \psi)\|_{|s|}^2.$$

This observation implies the existence and uniqueness of the solution by the Lax-Milgram lemma. In order to prove the stability bounds we first note that

$$|\mathcal{A}((v, \mathbf{u}, \psi), (w, \mathbf{w}, \varphi); s)| \leq C_1 \frac{|s|}{\underline{\sigma}} \|(w, \mathbf{w}, \varphi)\|_{|s|} \|(v, \mathbf{u}, \psi)\|_1, \quad (4.9)$$

$$\begin{aligned} |\ell((w, \mathbf{w}, \varphi); s)| &\leq \frac{C_2}{\underline{\sigma}} \|(w, \mathbf{w}, \varphi)\|_{|s|} \left(\|\alpha_d\|_{-1/2, \Gamma} + \|s\beta_d\|_{1/2, \Gamma} + \|\eta_d\|_{-1/2, \Gamma} \right. \\ &\quad \left. + \|s^2\boldsymbol{\theta}_d\|_{\Omega_-} + \|s\theta_d\|_{\Gamma} + \|\lambda_d\|_{-1/2, \Gamma} \right), \quad (4.10) \end{aligned}$$

where C_1 and C_2 depend only on the geometry, and in the second inequality we have employed (4.7) to bound the energy norm. Next, we pick liftings of the boundary data $\gamma^\dagger \phi_d \in H^1(\mathbb{R}^d \setminus \Gamma)$ and $\gamma_{h,D}^\dagger \mu_d^h \in V_h$ such that

$$\gamma^- \gamma^\dagger \phi_d = 0, \quad -\gamma^+ \gamma^\dagger \phi_d = \phi_d, \quad \|\gamma^\dagger \phi_d\|_{1, \Omega_-} \leq C \|\phi_d\|_{1/2, \Gamma}, \quad (4.11a)$$

$$\gamma \gamma_{h,D}^\dagger \mu_d^h = \mu_d^h, \quad \|\gamma_{h,D}^\dagger \mu_d^h\|_{1, \Omega_-} \leq C \|\mu_d^h\|_{1/2, \Gamma}. \quad (4.11b)$$

Since $\widehat{v}^h + \gamma^\dagger \phi_d \in V_h^*$ and $\widehat{\psi}^h + \gamma_{h,D}^\dagger \mu_d^h \in V_{h,D}$, we can use (4.5c) to show that

$$\|(\widehat{v}^h + \gamma^\dagger \phi_d, \widehat{\mathbf{u}}^h, \widehat{\psi}^h + \gamma_{h,D}^\dagger \mu_d^h)\|_{|s|}^2$$

$$\begin{aligned}
&\leq \frac{|s|}{\sigma} \left| \mathcal{A}((\widehat{v}^h + \gamma^\dagger \phi_d, \widehat{\mathbf{u}}^h, \widehat{\psi}^h + \gamma_{h,D}^\dagger \mu_d^h), (\widehat{v}^h + \gamma^\dagger \phi_d, \widehat{\mathbf{u}}^h, \widehat{\psi}^h + \gamma_{h,D}^\dagger \mu_d^h); s) \right| \\
&= \frac{|s|}{\sigma} \left| \ell((\widehat{v}^h + \gamma^\dagger \phi_d, \widehat{\mathbf{u}}^h, \widehat{\psi}^h + \gamma_{h,D}^\dagger \mu_d^h); s) \right. \\
&\quad \left. + \mathcal{A}((\gamma^\dagger \phi_d, \mathbf{0}, \gamma_{h,D}^\dagger \mu_d^h), (\widehat{v}^h + \gamma^\dagger \phi_d, \widehat{\mathbf{u}}^h, \widehat{\psi}^h + \gamma_{h,D}^\dagger \mu_d^h); s) \right| \\
&\leq \frac{|s|}{\sigma} \left\| (\widehat{v}^h + \gamma^\dagger \phi_d, \widehat{\mathbf{u}}^h, \widehat{\psi}^h + \gamma_{h,D}^\dagger \mu_d^h) \right\|_{|s|} \\
&\quad \times \left(\frac{C_2}{\underline{\sigma}} \left(\|\alpha_d\|_{-1/2,\Gamma} + \|s\beta_d\|_{1/2,\Gamma} + \|\eta_d\|_{-1/2,\Gamma} + \|s^2\boldsymbol{\theta}_d\|_{\Omega_-} \right. \right. \\
&\quad \left. \left. + \|s\theta_d\|_{\Gamma} + \|\lambda_d\|_{-1/2,\Gamma} \right) + C_1 \frac{|s|}{\underline{\sigma}} \left(\|\gamma^\dagger \phi_d\|_{1,\Omega_-} + \|\gamma_{h,D}^\dagger \mu_d^h\|_{1,\Omega_-} \right) \right) \\
&\leq C \frac{|s|}{\sigma \underline{\sigma}} \left\| (\widehat{v}^h + \gamma^\dagger \phi_d, \widehat{\mathbf{u}}^h, \widehat{\psi}^h + \gamma_{h,D}^\dagger \mu_d^h) \right\|_{|s|} A(\text{data}, s),
\end{aligned}$$

where (4.9), (4.10), and (4.11a) have been used. This implies

$$\left\| (\widehat{v}^h + \gamma^\dagger \phi_d, \widehat{\mathbf{u}}^h, \widehat{\psi}^h + \gamma_{h,D}^\dagger \mu_d^h) \right\|_{|s|} \leq C \frac{|s|}{\sigma \underline{\sigma}} A(\text{data}, s). \quad (4.12)$$

The inequality (4.8a) follows from (4.12) with an application of (4.7). The estimate (4.8b) can be derived from (4.12) by recalling that $\widehat{\lambda}^h = -\llbracket \partial_\nu \widehat{v}^h \rrbracket$ and applying [26, Lemma 15] which states that, if $\Delta v - s^2 v = 0$ in an open set \mathcal{O} with Lipschitz boundary, then

$$\|\partial_\nu v\|_{-1/2,\partial\mathcal{O}} \leq C \left(\frac{|s|}{\underline{\sigma}} \right)^{1/2} (\|sv\|_{\mathcal{O}} + \|\nabla v\|_{\mathcal{O}}). \quad (4.13)$$

This finishes the proof. \square

5 Time domain estimates

For the timed-domain estimates, data and solutions will be assumed to be in spaces of the form

$$W_+^k(\mathbf{X}) := \{ \xi \in C^{k-1}(\mathbb{R}; \mathbf{X}) : \xi \equiv 0 \text{ in } (-\infty, 0), \xi^{(k)} \in L^1(\mathbb{R}; \mathbf{X}) \},$$

for $k \geq 1$. We will also use the linear differential operator (cf. [14])

$$(\mathcal{P}_k f)(t) := \sum_{l=0}^k \binom{k}{l} f^{(l)}(t).$$

The stability bounds and semi-discrete error estimates obtained in the previous section can be translated into the following time-domain results. Taking the second group of data (4.1b) to be identically zero and setting

$$(\boldsymbol{\theta}_d, \theta_d, \lambda_d, \phi_d) = (\mathbf{P}_h \mathbf{u} - \mathbf{u}, \gamma(\mathbf{P}_h \mathbf{u} - \mathbf{u}) \cdot \boldsymbol{\nu}, \lambda, \phi),$$

an application of [14, Theorem 7.1] combined with Proposition 4.3 yields the following result

Corollary 5.1 (Stability in the time-domain). *Provided causal problem data*

$$(\alpha_d, \beta_d, \eta_d, \mu_d^h) \in W_+^3(H^{-1/2}(\Gamma)) \times W_+^4(H^{1/2}(\Gamma)) \times W_+^3(H^{-1/2}(\Gamma)) \times W_+^4(H^{1/2}(\Gamma))$$

then $\lambda^h, \phi^h, \mathbf{u}^h$ and ψ^h are continuous causal functions of time and there exist $D_1, D_2 > 0$ such that, for $t \geq 0$:

$$\begin{aligned} \|(v^h, \mathbf{u}^h, \psi^h)(t)\|_1 + \|\phi^h(t)\|_{1/2, \Gamma} &\leq \frac{D_1 t^2}{t+1} \max\{1, t^2\} \int_0^t \|\mathcal{P}_3(\dot{\alpha}_d, \beta_d, \eta_d, \dot{\mu}_d^h)(\tau)\|_{\pm 1/2, \Gamma} d\tau, \\ \|\lambda^h(t)\|_{-1/2, \Gamma} &\leq \frac{D_2 t^{3/2}}{\sqrt{t+1}} \max\{1, t^{3/2}\} \int_0^t \|\mathcal{P}_3(\dot{\alpha}_d, \beta_d, \eta_d, \dot{\mu}_d^h)(\tau)\|_{\pm 1/2, \Gamma} d\tau, \end{aligned}$$

where D_1 and D_2 depend only on Γ .

We introduce the approximation error

$$\begin{aligned} a_h(t) := &\int_0^t \left(\|\mathcal{P}_3(\dot{\phi} - \Pi_h^Y \dot{\phi})(\tau)\|_{1/2, \Gamma} + \|\mathcal{P}_3(\lambda - \Pi_h^X \lambda)(\tau)\|_{-1/2, \Gamma} \right) d\tau \\ &+ \int_0^t \left(\|\mathcal{P}_3(\ddot{\mathbf{u}} - \mathbf{P}_h \ddot{\mathbf{u}})(\tau)\|_{\Omega_-} + \|\mathcal{P}_3(\dot{\mathbf{u}} - \mathbf{P}_h \dot{\mathbf{u}})(\tau)\|_{1, \Omega_-} \right) d\tau, \end{aligned}$$

where Π_h^Y and Π_h^X are the orthogonal projections onto Y_h and X_h respectively, and \mathbf{P}_h is part of the elliptic projector defined in (3.11). Note that $\mathbf{P}_h \mathbf{u}$ depends on \mathbf{u} , ψ , and μ_d^h and that Lemma 3.1 states that

$$\|\mathbf{u} - \mathbf{P}_h \mathbf{u}\|_{1, \Omega_-} \leq C(\|\mathbf{u} - \Pi_V^h \mathbf{u}\|_{1, \Omega_-} + \|\psi - \Pi_V^h \psi\|_{1, \Omega_-} + \|\mu_d - \mu_d^h\|_{1/2, \Gamma}),$$

where Π_h^Y and Π_h^X are the respective H^1 best approximation operators on \mathbf{V}_h and V_h . Taking the data (4.1a) as in Proposition 4.3 and applying [14, Theorem 7.1] we can prove the following result

Corollary 5.2 (Semi-discrete error). *If the solution $(\lambda, \phi, \mathbf{u}, \psi)$ is causal and belongs to*

$$W_+^3(H^{-1/2}(\Gamma)) \times W_+^4(H^{1/2}(\Gamma)) \times [W_+^5(\mathbf{H}^1(\Omega_-)) \cap W_+^4(\mathbf{L}^2(\Omega_-))] \times [W_+^5(H^1(\Omega_-)) \cap W_+^4(L^2(\Omega_-))]$$

then, for every $t \geq 0$

$$\begin{aligned} \|(\mathbf{e}_v^h, \mathbf{e}_\mathbf{u}^h, e_\psi^h)(t)\|_1 + \|e_\phi^h(t)\|_{1/2, \Gamma} &\leq \frac{D_1 t^2}{t+1} \max\{1, t^2\} a_h(t), \\ \|(e_\lambda^h)(t)\|_{1/2, \Gamma} &\leq \frac{D_2 t^{3/2}}{\sqrt{t+1}} \max\{1, t^{3/2}\} a_h(t), \end{aligned}$$

where $D_1, D_2 > 0$ depend only on Γ ,

$$e_v^h := \mathcal{D} * (\phi - \phi^h) - \mathcal{S} * (\lambda - \lambda^h) = v - \mathbf{D} * \phi^h + \mathbf{S} * \lambda^h.$$

Here \mathcal{D} and \mathcal{S} are the operator-valued causal distributions whose Laplace transforms are $\mathbf{D}(s/c)$ and $\mathbf{S}(s/c)$, and $*$ is the symbol for distributional convolution in the time variable.

Convolution Quadrature and time-stepping. Convolution Quadrature (CQ) was developed by Christian Lubich in the late 80's and early 90's [19, 27, 28, 29] as a way to approximate causal convolutions and convolution equations based on the knowledge of the Laplace transform of the convolution kernel and time domain data.

Since then it has been enriched greatly by works like [34, 10, 18, 4, 5, 6, 7] and –due to its stability properties, the advantage of requiring only Laplace-domain fundamental solutions and the possibility to take damping effects into account with relative ease – has become one of the preferred tools for the numerical analysis and simulation of evolutionary problems arising from wave propagation and diffusion. A thorough review of results and properties of CQ applied to boundary integral equations can be found in [8], while [21] gives a detailed explanation of the computational and algorithmic subtleties involved in its implementation.

In the heart of every CQ implementation lies an ODE solver which determines its analytic and convergence properties and gives rise to different families of CQ algorithms. We will focus on BDF2 time-stepping for the analysis but will give numerical experiments for both BDF2 and Trapezoidal Rule-based methods. The integral equations will be treated numerically with CQ, while the Finite Element discretization of the elastic displacement and electric potential will be discretized in time using BDF2 and TR time-steppers.

The key result that will allow us to carry out all the time domain analysis using CQ based tools –even if our computational implementation involves traditional time stepping for the finite element discretization– is that this split treatment of different parts of a system is equivalent to the application of CQ globally, as long as the time stepping method used for the FEM part coincides with the one giving rise to the CQ algorithm in use (see [26, Proposition 12], [20]).

The approximation error between the fully discrete solution $(v_\kappa^h, \mathbf{u}_\kappa^h, \psi_\kappa^h)$ obtained using BDF2-CQ with a time step size κ and the semi-discrete approximation $(v^h, \mathbf{u}^h, \psi^h)$ can be estimated from Proposition 4.3 using [33, Proposition 4.6.1] (a slight variant of a result in [29]).

Corollary 5.3. *Let $\ell = 6$ and $(\alpha_d, \beta_d, \eta_d, \mu_d^h)$ be causal problem data satisfying*

$$(\alpha_d, \beta_d, \eta_d, \mu_d^h) \in W_+^{\ell+1}(H^{1/2}(\Gamma)) \times W_+^\ell(H^{-1/2}(\Gamma)) \times W_+^\ell(H^{-1/2}(\Gamma)) \times W_+^\ell(H^{1/2}(\Gamma)).$$

For $t \geq 0$, the difference between the semi-discrete solution and fully discrete solution obtained using BDF2-based Convolution Quadrature is bounded like

$$\|(v^h, \mathbf{u}^h, \psi^h)(t) - (v_\kappa^h, \mathbf{u}_\kappa^h, \psi_\kappa^h)(t)\|_1 \leq D(1 + t^2)\kappa^2 \int_0^t \|(\dot{\alpha}_d, \beta_d, \eta_0, \mu_0^h)^{(\ell)}(\tau)\|_\Gamma d\tau,$$

where D depends only on Γ . Reduced convergence of order $2/3$ is achieved for $\ell = 3$.

6 Numerical experiments

In order to test the convergence results proven in the previous section, the formulation was implemented using standard Lagrangian finite elements for the elastic and electric fields and Galerkin boundary elements for the acoustic field. We take \mathbf{V}_h and V_h to be

continuous \mathcal{P}_k finite elements on a triangular mesh of Ω_- . On the inherited mesh on Γ , we consider the space X_h of discontinuous piecewise \mathcal{P}_{k-1} and the space Y_h of continuous piecewise \mathcal{P}_k functions.

About the implementation. One of the advantages of the formulation we propose is that it lends itself to a highly modular implementation, in the sense that pre-existing FEM code for piezoelectricity and BEM code for acoustics can be used to solve the coupled problem in the frequency domain without any modification. The only requirement is the addition of a “discrete trace” which translates boundary FEM degrees of freedom into BEM degrees of freedom. Formally, the structure of the discrete system (3.9) can be represented as

$$\begin{pmatrix} \mathbf{FEM}(s) & s\rho_f(\mathbf{N}\Gamma)_h^\top \\ -s\rho_f(\mathbf{N}\Gamma)_h & \rho_f\mathbf{BEM}(s) \end{pmatrix} \begin{pmatrix} \begin{pmatrix} \mathbf{u}^h \\ \psi^h \end{pmatrix} \\ \begin{pmatrix} \lambda^h \\ \phi^h \end{pmatrix} \end{pmatrix} = \begin{pmatrix} \begin{pmatrix} -s\rho_f\Gamma_h^\top\beta^h \\ \eta^h \end{pmatrix} \\ \begin{pmatrix} 0 \\ \rho_f\alpha^h \end{pmatrix} \end{pmatrix},$$

where: (a) the finite element block $\mathbf{FEM}(s)$ contains sparse s -independent elastic stiffness, material mass, piezoelectric, and electric stiffness-like matrices, the material mass matrix being multiplied by s^2 (see (3.8a) and (3.8b)); (b) the boundary element block $\mathbf{BEM}(s)$ contains Galerkin discretizations of the operators of the Calderón projector (see (3.8c)); (c) the sparse matrix $(\mathbf{N}\Gamma)_h$ corresponds to the discretization of the bilinear form $\mathbf{V}_h \times Y_h \ni (\mathbf{u}^h, \chi^h) \mapsto \langle \mathbf{u}^h \cdot \boldsymbol{\nu}, \chi^h \rangle_\Gamma$ with added zero blocks for the interactions of all other spaces. We note that the trace space for \mathbf{V}_h is a vector-valued version of Y_h , which means that, apart from rearrangements of degrees of freedom (and possible changes of local polynomial bases), the only matrix connecting the BEM and FEM codes is simple to implement.

In a similar way, the transition from Laplace domain to time domain can be done in a modularly, either by implementing a CQ routine that inverts the full operator matrix, or a time stepping routine where s is replaced with a discrete approximation of the differentiation operator, or using a Schur complement strategy as was first suggested in [3] and outlined in [20] for a purely acoustic system or as in [22] for a coupled acoustic/elastic problem. The latter approach, which results in a decoupling of the boundary integral part of the system, is well suited for parallelization and was the chosen strategy for the following numerical experiments.

Geometric setup and physical parameters. In all the convergence studies (frequency and time domain), the rectangle $\Omega_- := (1, 3) \times (1, 2) \subset \mathbb{R}^2$ was used as the piezoelectric domain. The double-indices used in our general presentation of tensor in the piezoelectric domains will be reduced to a single index using the simple convention:

$$(1, 1) \leftrightarrow 1 \quad (2, 2) \leftrightarrow 2 \quad (1, 2) \leftrightarrow 3.$$

(By symmetry, the pair (2,1) can be avoided in the tensor representations.) We choose the following constant Lamé parameters, mass density, and acoustic speed of sound:

$$\lambda = 2, \quad \mu = 3, \quad \rho = 5, \quad c = 1. \quad (6.1a)$$

We will use Young's modulus and Poisson's ratio

$$E := \frac{2\mu(1+\lambda)}{2\mu+\lambda}, \quad \nu := \frac{\lambda}{2\mu+\lambda} \quad (6.1b)$$

to express the entries of the elastic compliance tensor \mathbf{C}

$$\mathbf{C}_{11} = \mathbf{C}_{22} = \frac{E}{1-\nu^2}, \quad \mathbf{C}_{33} = \frac{E}{2(1+\nu)}, \quad \mathbf{C}_{12} = \frac{E\nu}{1-\nu^2}, \quad \mathbf{C}_{13} = \mathbf{C}_{23} = 0. \quad (6.1c)$$

For the piezoelectric tensor \mathbf{e} the values used were

$$\mathbf{e}_{11} = \mathbf{e}_{22} = \mathbf{e}_{33} = 1, \quad \mathbf{e}_{12} = \mathbf{e}_{13} = \mathbf{e}_{23} = 5, \quad (6.1d)$$

while for the dielectric tensor $\boldsymbol{\epsilon}$ the entries were

$$\boldsymbol{\epsilon}_{11} = \boldsymbol{\epsilon}_{22} = 4, \quad \boldsymbol{\epsilon}_{12} = 1. \quad (6.1e)$$

We take $\Gamma_D = \Gamma$ and $\Gamma_N = \emptyset$.

Convergence studies in the frequency domain. The elastic plane pressure wave

$$\mathbf{u}(\mathbf{x}) = e^{-sc_L \mathbf{x} \cdot \mathbf{d}}, \quad \mathbf{d} = \left(\frac{1}{\sqrt{2}}, \frac{1}{\sqrt{2}} \right), \quad c_L = \sqrt{\frac{2\mu+\lambda}{\rho}}$$

with $s = -2.5i$ was imposed as a solution alongside the electric field

$$\psi(\mathbf{x}) = x_1^3 + x_1^3 x_2 - 3x_1 x_2^2 - \frac{1}{3} x_2^3.$$

In the acoustic domain, the cylindrical acoustic wave

$$v(\mathbf{x}) = \frac{i}{4} H_0^{(1)}(is|\mathbf{x} - \mathbf{x}_0|), \quad \mathbf{x}_0 = (2, 1.5) \in \Omega_-$$

was used. Right-hand sides are added to equations (3.1b) and (3.1c)

$$\nabla \cdot \boldsymbol{\sigma} = \rho_\Sigma s^2 \mathbf{u} + f_1 \quad \nabla \cdot \mathbf{D} = f_2$$

so that (\mathbf{u}, ψ) is a solution. Note that both f_1 and f_2 are independent of the frequency s , due to the fact that we have chosen \mathbf{u} to be an elastic plane wave. Boundary data for ψ and transmission data in (3.1d)-(3.1e) are built so that the equations are satisfied.

The experiment was ran using $k = 1, 2$ for the \mathcal{P}_k finite elements and $\mathcal{P}_k/\mathcal{P}_{k-1}$ boundary elements. The acoustic wave was sampled in twenty random points in the exterior of the piezoelectric domain and compared to the exact solution, using the maximum discrepancy as the measure of the acoustic error E_h^v . For the elastic and electric unknowns both $L^2(\Omega_-)$ and $H^1(\Omega_-)$ errors were computed. Tables 1 and 2 as well as Figure 2 show the outcome of the convergence tests.

$k = 1$			$L^2(\Omega_-)$				$H^1(\Omega_-)$			
h	E_h^v	e.c.r.	E_h^u	e.c.r.	E_h^ψ	e.c.r.	E_h^u	e.c.r.	E_h^ψ	e.c.r.
0.2	7.110 E-2	—	1.167 E-1	—	4.140 E-2	—	7.835 E-1	—	1.718	—
0.1	1.760 E-2	2.014	3.146 E-2	1.891	1.047 E-2	1.984	2.646 E-1	1.566	8.544 E-1	1.007
0.05	4.615 E-3	1.931	8.138 E-3	1.951	2.632 E-3	1.991	9.372 E-2	1.497	4.263 E-1	1.003
0.025	1.171 E-3	1.978	2.059 E-3	1.983	6.599 E-4	1.996	3.734 E-2	1.327	2.130 E-1	1.001

Table 1: Relative errors and estimated convergence rates in the time frequency domain with \mathcal{P}_1 finite elements and $\mathcal{P}_1/\mathcal{P}_0$ boundary elements. h represents the maximum length of the panels used to discretize the boundary.

$k = 2$			$L^2(\Omega_-)$				$H^1(\Omega_-)$			
h	E_h^v	e.c.r.	E_h^u	e.c.r.	E_h^ψ	e.c.r.	E_h^u	e.c.r.	E_h^ψ	e.c.r.
0.2	5.545 E-5	—	3.542 E-4	—	3.927 E-4	—	1.350 E-2	—	1.805 E-2	—
0.1	4.161 E-6	3.736	3.949 E-5	3.024	4.872 E-5	3.024	3.083 E-3	2.130	4.450 E-3	2.020
0.05	3.146 E-7	3.725	4.555 E-6	3.116	5.991 E-6	3.010	7.153 E-4	2.108	1.105 E-3	2.009
0.025	2.379 E-8	3.725	5.455 E-7	3.062	7.463 E-7	3.005	1.710 E-4	2.064	2.753 E-4	2.005

Table 2: Relative errors and estimated convergence rates in the time frequency domain with \mathcal{P}_2 finite elements and $\mathcal{P}_2/\mathcal{P}_1$ boundary elements. h represents the maximum length of the panels used to discretize the boundary.

Convergence studies in the time domain. Experiments were carried out using matching time stepping (for the FEM part) and CQ (for the BEM part) based on both Trapezoidal Rule and BDF2 for time evolution. The fully discrete method based on the trapezoidal rule can be analyzed in the same way as BDF2, using results from [4]. Note that the only difference is the lack of knowledge of how the error constants depend on the time variable.

Just as in the frequency domain case, the rectangle $\Omega_- := (1, 3) \times (1, 2) \subset \mathbb{R}^2$ was used as the piezoelectric domain where the elastic plane pressure wave

$$\mathbf{u}(\mathbf{x}, t) = \mathcal{H}(c_L t - \mathbf{x} \cdot \mathbf{d}) \sin(3(c_L t - \mathbf{x} \cdot \mathbf{d})) \mathbf{d}, \quad \mathbf{d} = \left(\frac{1}{\sqrt{2}}, \frac{1}{\sqrt{2}} \right), \quad c_L = \sqrt{\frac{2\mu + \lambda}{\rho}},$$

and the causal electric field

$$\psi(\mathbf{x}, t) = \mathcal{H}(t)(x_1^3 + x_1^3 x_2 - 3x_1 x_2^2 - \frac{1}{3}x_2^3),$$

were imposed. In the acoustic domain, the cylindrical acoustic wave

$$v(\mathbf{x}, t) = \mathcal{L}^{-1} \left\{ iH_0^{(1)}(i s |\mathbf{x} - \mathbf{x}_0|) \mathcal{L}\{\mathcal{H}(t) \sin(2t)\} \right\},$$

centered at $\mathbf{x}_0 = (2, 1.5)$, was imposed. In all cases \mathcal{H} is the piecewise polynomial approximation to Heaviside's step function

$$\mathcal{H}(t) := t^5(1 - 5(t - 1) + 15(t - 1)^2 - 35(t - 1)^3 + 70(t - 1)^4 - 126(t - 1)^5)\chi_{[0,1]} + \chi_{[1,\infty)}.$$

Analogously to the frequency domain experiments, right hand sides were added so that (\mathbf{u}, ψ) are solutions to the system and the appropriate Dirichlet data was sampled at the boundary using Equations (2.3d), (2.3e), and (2.3g) to define the boundary data.

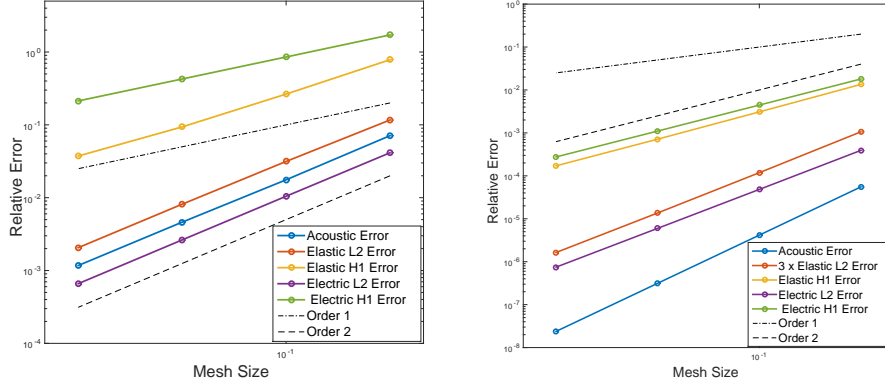


Figure 2: Convergence studies for the frequency domain problem are shown for $\mathcal{P}_1/\mathcal{P}_0$ boundary elements and \mathcal{P}_1 finite elements (left) and $\mathcal{P}_2/\mathcal{P}_1$ boundary elements and \mathcal{P}_2 finite elements (right).

The experiment was ran using $k = 1, 2$ for the \mathcal{P}_k finite elements and $\mathcal{P}_k/\mathcal{P}_{k-1}$ boundary elements. The time step and mesh size were refined simultaneously and the final time was $t = 1.5$. All errors are measured at the final time: $E_{h,\kappa}^v$ measures the maximum error on twenty randomly chosen points in the exterior domain, while elastic and electric fields errors are measured in the $L^2(\Omega_-)$ and $H^1(\Omega_-)$ norms. Tables 3 and 4 along with Figure 3 show the outcome of the convergence tests.

$k = 1$			$L^2(\Omega_-)$				$H^1(\Omega_-)$			
h/κ	$E_{h,\kappa}^v$	e.c.r.	$E_{h,\kappa}^u$	e.c.r.	$E_{h,\kappa}^\psi$	e.c.r.	$E_{h,\kappa}^u$	e.c.r.	$E_{h,\kappa}^\psi$	e.c.r.
2 E-1/7.5 E-2	2.054 E-2	—	6.363 E-2	—	4.179 E-2	—	5.714 E-1	—	1.702	—
1 E-1/3.75 E-2	7.864 E-3	1.385	1.726 E-2	1.882	1.034 E-2	2.015	2.067 E-1	1.467	8.515 E-1	0.999
5 E-2/1.875 E-2	1.831 E-3	2.102	4.537 E-3	1.928	2.590 E-3	1.997	8.600 E-2	1.265	4.258 E-1	1.000
2.5 E-2/9.375 E-3	4.485 E-4	2.030	1.159 E-3	1.969	6.485 E-4	1.997	3.912 E-2	1.136	2.129 E-1	1.000

Table 3: Relative errors and estimated convergence rates in the time domain for the Trapezoidal Rule Convolution Quadrature with \mathcal{P}_1 finite elements and $\mathcal{P}_1/\mathcal{P}_0$ boundary elements: h represents the maximum length of the panels used to discretize the boundary, κ is the size of the timesteps. The errors are measured at the final time $T = 1.5$.

$k = 2$			$L^2(\Omega_-)$				$H^1(\Omega_-)$			
h/κ	$E_{h,\kappa}^v$	e.c.r.	$E_{h,\kappa}^u$	e.c.r.	$E_{h,\kappa}^\psi$	e.c.r.	$E_{h,\kappa}^u$	e.c.r.	$E_{h,\kappa}^\psi$	e.c.r.
2 E-1/7.5 E-2	3.422 E-2	—	4.627 E-2	—	1.544 E-2	—	6.323 E-1	—	1.495 E-1	—
1 E-1/3.75 E-2	2.329 E-2	0.555	1.242 E-2	1.898	3.722 E-3	2.052	1.821 E-1	1.795	3.260 E-2	2.197
5 E-2/1.875 E-2	5.836 E-3	1.997	3.128 E-3	1.989	9.194 E-4	2.017	4.607 E-2	1.983	7.735 E-3	2.076
2.5 E-2/9.375 E-3	1.444 E-3	2.015	7.826 E-4	1.999	2.288 E-4	2.007	1.151 E-2	2.001	1.907 E-3	2.020

Table 4: Relative errors and estimated convergence rates in the time domain for the Trapezoidal Rule Convolution Quadrature with \mathcal{P}_2 finite elements and $\mathcal{P}_2/\mathcal{P}_1$ boundary elements: h represents the maximum length of the panels used to discretize the boundary, κ is the size of the timesteps. The errors are measured at the final time $T = 1.5$.

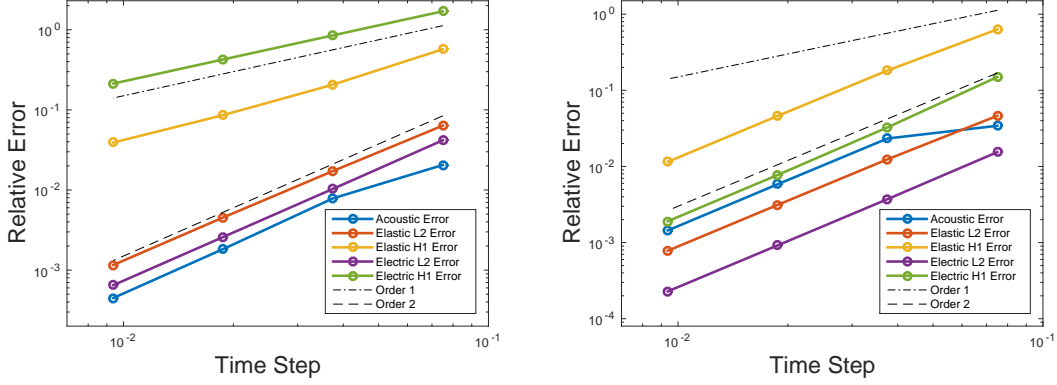


Figure 3: Convergence studies for the Trapezoidal Rule-based time stepping in the case of $\mathcal{P}_1/\mathcal{P}_0$ boundary elements and \mathcal{P}_1 finite elements (left) and $\mathcal{P}_2/\mathcal{P}_1$ boundary elements and \mathcal{P}_2 finite elements (right).

$k = 1$			$L^2(\Omega_-)$				$H^1(\Omega_-)$			
h/κ	$E_{h,\kappa}^v$	e.c.r.	$E_{h,\kappa}^u$	e.c.r.	$E_{h,\kappa}^\psi$	e.c.r.	$E_{h,\kappa}^u$	e.c.r.	$E_{h,\kappa}^\psi$	e.c.r.
2 E-1/7.5 E-2	2.805 E-2	—	9.448 E-2	—	4.772 E-2	—	7.683 E-1	—	1.709	—
1 E-1/3.75 E-2	2.543 E-2	0.141	3.401 E-2	1.474	1.377 E-2	1.793	3.931 E-1	0.967	8.546 E-1	1.000
5 E-2/1.875 E-2	1.571 E-2	0.694	1.010 E-2	1.749	3.689 E-3	1.900	1.513 E-1	1.378	4.264 E-1	1.003
2.5 E-2/9.375 E-3	4.650 E-3	1.757	2.655 E-3	1.930	9.379 E-4	1.975	5.231 E-2	1.532	2.130 E-1	1.001

Table 5: Relative errors and estimated convergence rates in the time domain for the BDF2-based Convolution Quadrature with \mathcal{P}_1 finite elements and $\mathcal{P}_1/\mathcal{P}_0$ boundary elements: h represents the maximum length of the panels used to discretize the boundary, κ is the size of the timesteps. The errors are measured at the final time $T = 1.5$.

A sample simulation. As an example, we consider the interaction between the acoustic pulse

$$v^{inc} = 3\chi_{[0,0.3]}(88s) \sin(88s), \quad s := (t - \mathbf{r} \cdot \mathbf{d}), \quad \mathbf{r} := (x, y), \quad \mathbf{d} := (1, 5)/\sqrt{26},$$

and a pentagonal piezoelectric scatterer with mass density given by

$$\rho = 5 + 25e^{-(10|\mathbf{r}|)^2}.$$

The remaining physical parameters of the solid were taken to be those defined by (6.1) and the entire solid/fluid interface was taken as Dirichlet boundary, where a grounding potential $\psi \equiv 0$ was imposed as boundary condition for all times. The simulation was carried out using \mathcal{P}_2 Lagrangian finite elements and $\mathcal{P}_2/\mathcal{P}_1$ continuous/discontinuous Galerkin boundary elements with Trapezoidal Rule-based time discretization using a time step $\kappa = 0.005$. Figures 5 to 7 show snapshots of the process at different times.

7 Conclusions

We have developed a well-posed integro-differential formulation for the interaction of acoustic waves and piezoelectric scatterers with Lipschitz boundaries in the transient

$k = 2$			$L^2(\Omega_-)$				$H^1(\Omega_-)$			
h/κ	$E_{h,\kappa}^v$	e.c.r.	$E_{h,\kappa}^u$	e.c.r.	$E_{h,\kappa}^\psi$	e.c.r.	$E_{h,\kappa}^u$	e.c.r.	$E_{h,\kappa}^\psi$	e.c.r.
2 E-1/7.5 E-2	2.959 E-2	—	9.368 E-2	—	2.999 E-2	—	8.178 E-1	—	2.287 E-1	—
1 E-1/3.75 E-2	3.047 E-2	-0.041	3.884 E-2	1.270	1.247 E-2	1.265	4.699 E-1	0.799	1.097 E-1	1.059
5 E-2/1.875 E-2	1.958 E-2	0.638	1.186 E-2	1.712	3.566 E-3	1.806	1.664 E-1	1.498	3.084 E-3	1.832
2.5 E-2/9.375 E-3	5.680 E-3	1.785	3.099 E-3	1.936	9.102 E-4	1.970	4.511 E-2	1.883	7.617 E-3	2.018

Table 6: Relative errors and estimated convergence rates in the time domain for the BDF2-based Convolution Quadrature with \mathcal{P}_2 finite elements and $\mathcal{P}_2/\mathcal{P}_1$ boundary elements: h represents the maximum length of the panels used to discretize the boundary, κ is the size of the timesteps. The errors are measured at the final time $T = 1.5$.

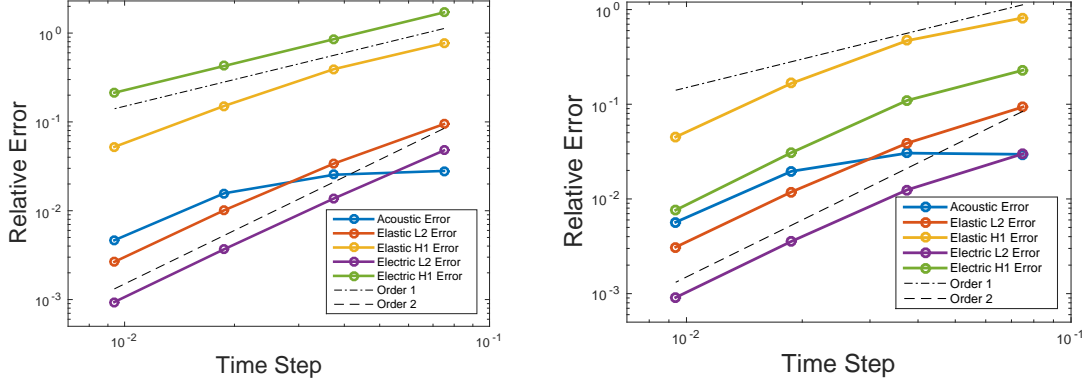


Figure 4: Convergence studies for the BDF2-based time stepping in the case of $\mathcal{P}_1/\mathcal{P}_0$ boundary elements and \mathcal{P}_1 finite elements (left) and $\mathcal{P}_2/\mathcal{P}_1$ boundary elements and \mathcal{P}_2 finite elements (right).

regime. The formulation is geared towards a numerical implementation employing boundary elements for the acoustic field in the unbounded exterior domain and finite elements for the elastic and electric fields inside of the bounded scatterer, and can be easily implemented computationally building on existing FEM and BEM routines.

We have shown that the resulting stability bounds in the Laplace domain can be used to give explicit time-domain error bounds when BDF2-CQ is used for time discretization, resulting in a quasi-optimal in time scheme of order 2 for sufficiently smooth problem data. Numerical evidence strongly suggests that the Trapezoidal Rule based method has the same optimal convergence order and in fact may have better numerical properties such as a much shorter pre-asymptotic regime and smaller error constants than those for BDF2.

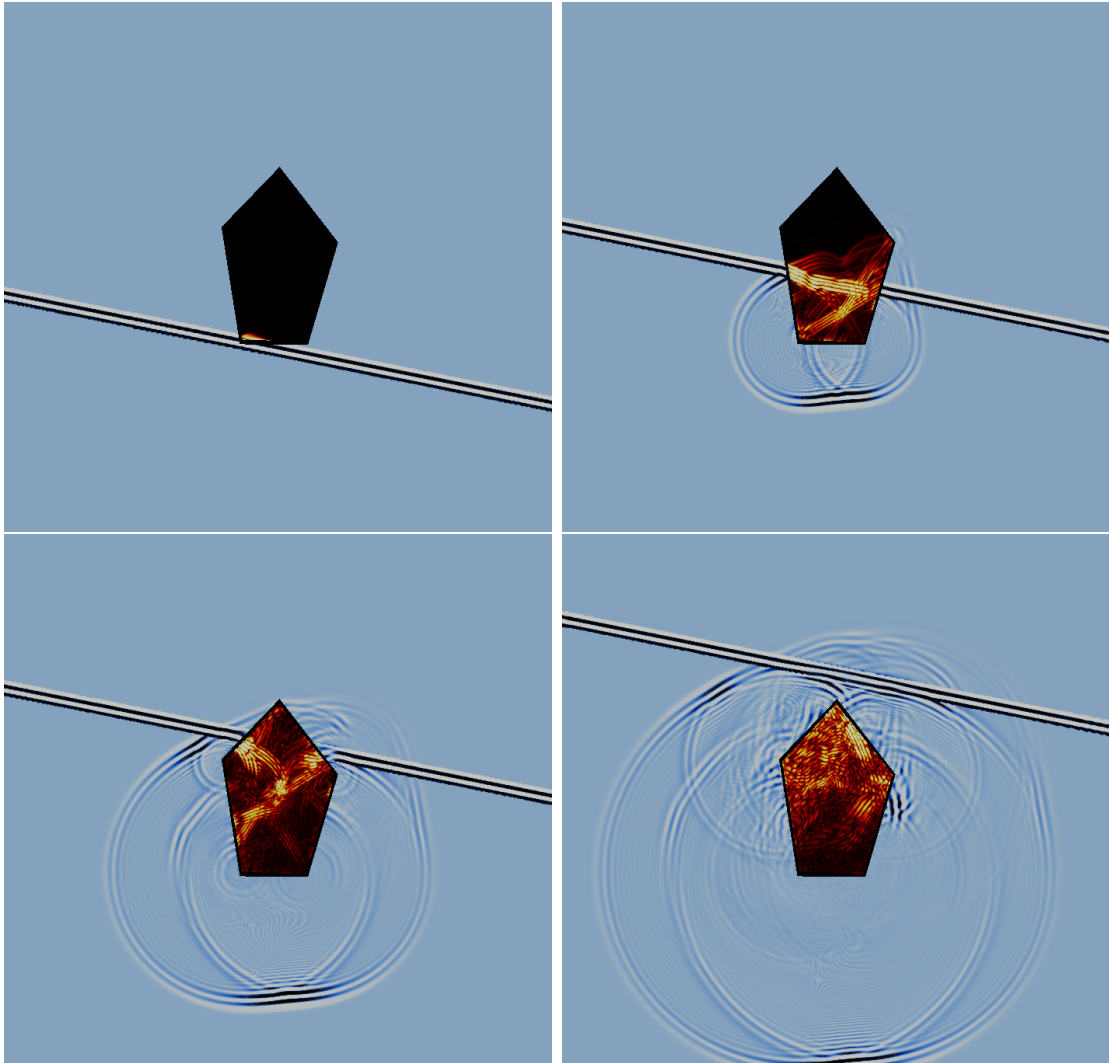


Figure 5: The total acoustic wave shown at times $t = 0.175, 0.7, 1.225, 1.75$.

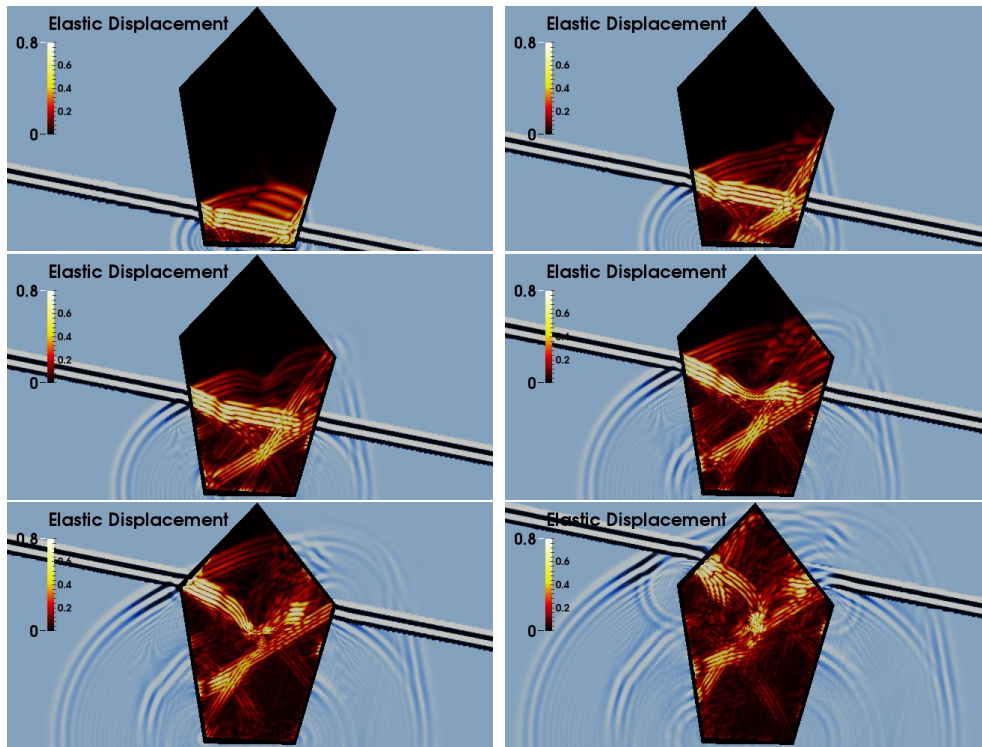


Figure 6: Close up of the norm of the elastic displacement at times $t = 0.35, 0.525, 0.7, 0.875, 1.05, 1.225$.

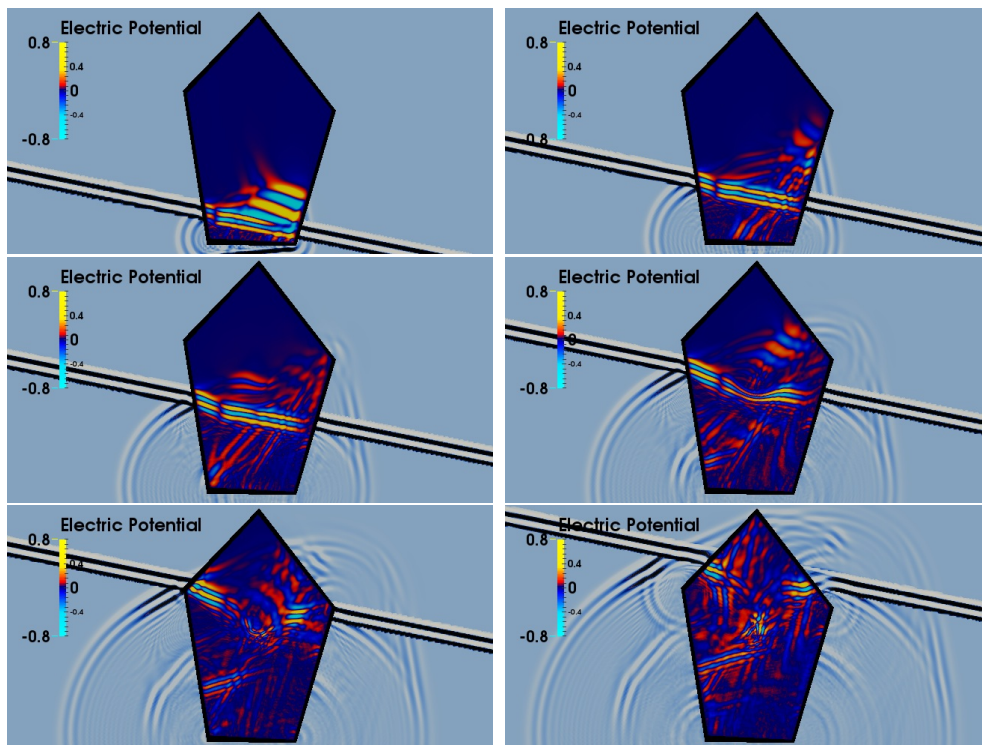


Figure 7: Close up of the electric potential at times $t = 0.35, 0.525, 0.7, 0.875, 1.05, 1.225$.

References

- [1] Henno Allik and Thomas J. R. Hughes. Finite element method for piezoelectric vibration. *Internat. J. Numer. Methods Engrg.*, 2(2):151–157, 1970.
- [2] A. Bamberger and T. Ha Duong. Formulation variationnelle espace-temps pour le calcul par potentiel retardé de la diffraction d’une onde acoustique. I. *Math. Methods Appl. Sci.*, 8(3):405–435, 1986.
- [3] L. Banjai and S. Sauter. Rapid solution of the wave equation in unbounded domains. *SIAM J. Numer. Anal.*, 47(1):227–249, 2008/09.
- [4] Lehel Banjai. Multistep and multistage convolution quadrature for the wave equation: algorithms and experiments. *SIAM J. Sci. Comput.*, 32(5):2964–2994, 2010.
- [5] Lehel Banjai and Christian Lubich. An error analysis of Runge-Kutta convolution quadrature. *BIT*, 51(3):483–496, 2011.
- [6] Lehel Banjai, Christian Lubich, and Jens Markus Melenk. Runge-Kutta convolution quadrature for operators arising in wave propagation. *Numer. Math.*, 119(1):1–20, 2011.
- [7] Lehel Banjai, Christian Lubich, and Francisco-Javier Sayas. Stable numerical coupling of exterior and interior problems for the wave equation. *Numer. Math.*, 129(4):611–646, 2015.
- [8] Lehel Banjai and Martin Schanz. Wave propagation problems treated with convolution quadrature and BEM. In *Fast boundary element methods in engineering and industrial applications*, volume 63 of *Lect. Notes Appl. Comput. Mech.*, pages 145–184. Springer, Heidelberg, 2012.
- [9] A. Benjeddou. Advances in piezoelectric finite element modeling of adaptive structural elements: a survey. *Computers & Structures*, 76(1–3):347 – 363, 2000.
- [10] M. P. Calvo, E. Cuesta, and C. Palencia. Runge-Kutta convolution quadrature methods for well-posed equations with memory. *Numer. Math.*, 107(4):589–614, 2007.
- [11] J.-F. Deü, W. Larbi, and R. Ohayon. Piezoelectric structural acoustic problems: Symmetric variational formulations and finite element results. *Comput. Methods Appl. Mech. Engrg.*, 197(19–20):1715 – 1724, 2008. Computational Methods in Fluid–Structure Interaction.
- [12] Jean-François Deü, Walid Larbi, and Roger Ohayon. Variational formulations of interior structural-acoustic vibration problems. In Göran Sandberg and Roger Ohayon, editors, *Computational Aspects of Structural Acoustics and Vibration*, volume 505 of *CISM International Centre for Mechanical Sciences*, pages 1–21. Springer Vienna, 2009.
- [13] Víctor Domínguez and Francisco-Javier Sayas. Stability of discrete liftings. *C. R. Math. Acad. Sci. Paris*, 337(12):805–808, 2003.

- [14] Víctor Domínguez and Francisco-Javier Sayas. Some properties of layer potentials and boundary integral operators for the wave equation. *J. Integral Equations Appl.*, 25(2):253–294, 2013.
- [15] M. Enderlein, A. Ricoeur, and M. Kuna. Finite element techniques for dynamic crack analysis in piezoelectrics. *International Journal of Fracture*, 134(3-4):191–208, 2005.
- [16] Felipe García-Sánchez, Chuanzeng Zhang, and Andrés Sáez. 2-D transient dynamic analysis of cracked piezoelectric solids by a time-domain BEM. *Comput. Methods Appl. Mech. Engrg.*, 197(33–40):3108 – 3121, 2008.
- [17] L. Gaul, M. Kögl, F. Moser, and M. Schanz. *Boundary Element Methods for the Dynamic Analysis of Elastic, Viscoelastic, and Piezoelectric Solids*. John Wiley & Sons, Ltd, 2004.
- [18] Wolfgang Hackbusch, Wendy Kress, and Stefan A. Sauter. Sparse convolution quadrature for time domain boundary integral formulations of the wave equation. *IMA J. Numer. Anal.*, 29(1):158–179, 2009.
- [19] E. Hairer, Ch. Lubich, and M. Schlichte. Fast numerical solution of nonlinear Volterra convolution equations. *SIAM J. Sci. Statist. Comput.*, 6(3):532–541, 1985.
- [20] M. Hassell and F.-J. Sayas. A fully discrete BEM-FEM scheme for transient acoustic waves. Submitted. arXiv:1601.08248 [math.NA], 2016.
- [21] Matthew Hassell and Francisco-Javier Sayas. *Convolution Quadrature for Wave Simulations*. Springer SEMA-SIMAI Lecture Notes in Mathematics, 2016. To appear.
- [22] George Hsiao, Tonatiuh Sánchez-Vizuet, and Francisco-Javier Sayas. Boundary and coupled boundary-finite element methods for transient wave-structure interaction. *IMA J. Numer. Anal.*, 2016. To appear.
- [23] Frank Ihlenburg. *Finite element analysis of acoustic scattering*, volume 132 of *Applied Mathematical Sciences*. Springer-Verlag, New York, 1998.
- [24] M. Kögl and L. Gaul. A boundary element method for transient piezoelectric analysis. *Engineering Analysis with Boundary Elements*, 24(7–8):591 – 598, 2000.
- [25] M. Kögl and L. Gaul. Piezoelectric analysis with FEM and BEM. In Afzal Suleman, editor, *Smart Structures*, volume 429 of *International Centre for Mechanical Sciences*, pages 120–130. Springer Vienna, 2001.
- [26] Antonio R. Laliena and Francisco-Javier Sayas. Theoretical aspects of the application of Convolution Quadrature to scattering of acoustic waves. *Numer. Math.*, 112(4):637–678, 2009.
- [27] C. Lubich. Convolution quadrature and discretized operational calculus. I. *Numer. Math.*, 52(2):129–145, 1988.

- [28] C. Lubich. Convolution quadrature and discretized operational calculus. II. *Numer. Math.*, 52(4):413–425, 1988.
- [29] Ch. Lubich. On the multistep time discretization of linear initial-boundary value problems and their boundary integral equations. *Numer. Math.*, 67(3):365–389, 1994.
- [30] H. Nguyen-Vinh, I. Bakar, M.A. Msekh, J.-H. Song, J. Muthu, G. Zi, P. Le, S.P.A. Bordas, R. Simpson, S. Natarajan, T. Lahmer, and T. Rabczuk. Extended finite element method for dynamic fracture of piezo-electric materials. *Engineering Fracture Mechanics*, 92:19 – 31, 2012.
- [31] Ernian Pan. A BEM analysis of fracture mechanics in 2D anisotropic piezoelectric solids. *Engineering Analysis with Boundary Elements*, 23(1):67 – 76, 1999.
- [32] Yu Pang, Yue-Sheng Wang, Jin-Xi Liu, and Dai-Ning Fang. Reflection and refraction of plane waves at the interface between piezoelectric and piezomagnetic media. *International Journal of Engineering Science*, 46(11):1098 – 1110, 2008.
- [33] Francisco-Javier Sayas. *Retarded potentials and time domain integral equations: a roadmap*, volume 50 of *Computational Mathematics*. Springer, 2016.
- [34] Achim Schädle, María López-Fernández, and Christian Lubich. Fast and oblivious convolution quadrature. *SIAM J. Sci. Comput.*, 28(2):421–438 (electronic), 2006.
- [35] H. F. Tiersten. *Linear piezoelectric plate vibrations*. Springer, 1969.
- [36] X. Yuan and Z.H. Zhu. Reflection and refraction of plane waves at interface between two piezoelectric media. *Acta Mechanica*, 223(12):2509–2521, 2012.
- [37] Peng Zhao, Taiyan Qin, and Linnan Zhang. A regularized time-domain BIEM for transient elastodynamic crack analysis in piezoelectric solids. *Engineering Analysis with Boundary Elements*, 56:145 – 153, 2015.